# Tight Bounds on 3-Neighbor Bootstrap Percolation

by

Abel Emanuel Romer
B.A.Sc., Quest University Canada, 2017

A Thesis Submitted in Partial Fulfillment of the
Requirements for the Degree of

MASTER OF SCIENCE

in the Department of Mathematics and Statistics



We acknowledge with respect the Lekwungen peoples on whose traditional territory the university stands, and the Songhees, Esquimalt, and W̱SÁNEĆ peoples whose historical relationships with the land continue to this day.

Tight Bounds on 3-Neighbor Bootstrap Percolation

by

Abel Emanuel Romer
B.A.Sc., Quest University Canada, 2017

Supervisory Committee

Dr. Peter Dukes, Co-Supervisor
(Department of Mathematics and Statistics)

Dr. Jonathan Noel, Co-Supervisor
(Department of Mathematics and Statistics)

## ABSTRACT

# Table of Contents

# List of Tables

# List of Figures

# ACKNOWLEDGEMENTS

# DEDICATION

# Chapter 1
# Introduction

Consider the lattice depicted in the leftmost diagram of Figure 1.1. We refer to the elements of this lattice as *cells*. Suppose we have the capacity to infect some cells (colored red) with a disease, and that this disease will, over a period of time, propagate through uninfected cells of the lattice. Let uninfected cells become infected if they are exposed to at least two infected neighboring cells in the vertical and/or horizontal directions. We say that the initial infection is *lethal* if the entire lattice ultimately becomes infected. Here is a puzzle:

**Question.** *What is the fewest number of infected cells necessary to spawn a lethal infection?*

Before we present the solution, let us take a moment to examine some properties of infectious sets and attempt to characterize what attributes might correspond to lethality. It should not take too long to observe that if an initial infection is in some way "spread too thinly," then it will be unable to "jump" between infected areas, leading to gaps in infection, which we refer to as *immune regions*. The perimeter of the lattice is particularly susceptible to this, as vertices there have fewer neighbors from whom they might be exposed. Heuristically, then, a lethal set must have the ability to effectively span the entire lattice, and must be particularly virulent along the perimeter.

With this criteria in mind, we are able to make some educated guesses regarding the specific structure of sets that are likely to be lethal. In particular, we would like to

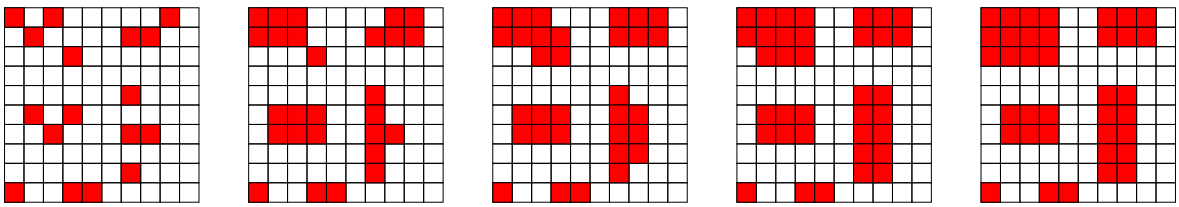

Figure 1.1: An arbitrary set of initially infected cells in the $10 \times 10$ lattice, and the stages of infection.

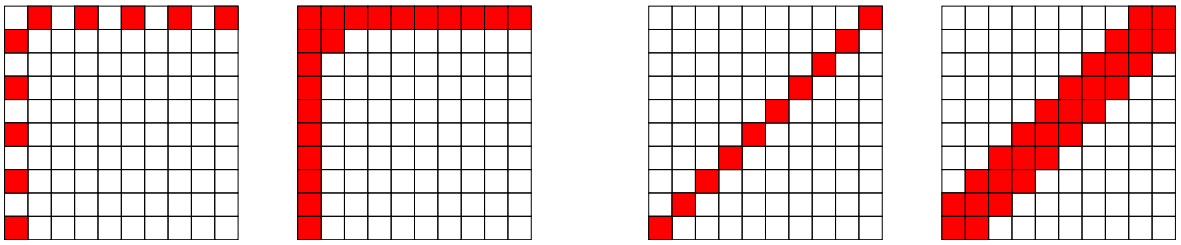

(a) Perimeter construction. (b) Diagonal construction.

Figure 1.2: Two lethal sets and their resulting infections after one time-step.

consider the two starting infections illustrated in Figure 1.2. Notice that while Figure 1.2 (b) has far fewer perimeter infections, both (a) and (b) manage to form continuous bands of infected cells that appear to span the entire lattice after one step. Indeed, this fits with our notion of immune regions (or lack thereof), and we see that both infections will continue to propagate outwards from these bands until all cells become infected.

It is clear from Figure 1.2 that we may obtain lethal sets on the $n \times n$ lattice of size $n$ by simply infecting the diagonal. What is less obvious is whether it is possible to improve upon this result. Perhaps the most natural first attempt at this is to remove an infection from one of the cells along the diagonal. However, this seems to form an immune region containing the removed cell. After some experimentation, one begins to believe it impossible to simultaneously satisfy the heuristic that a starting infection must span the lattice, while also using fewer than $n$ initial infections. The question therefore becomes: how do we prove it?

### An early result

Consider the cumulative perimeter of infected regions. For a given infectious set $A$, let $P(A)$ be the total perimeter of the infected regions of $A$. Let $A_0$ be an initial infection, and observe that $P(A_0) \leq 4|A_0|$. (This bound is only tight if no two infected cells are adjacent. Otherwise, the edge between such cells lies within the infected region, and cannot contribute to the infection's perimeter.) Observe that for any uninfected cell to become infected, it must abut at least two infected cells. Upon infection, the edges adjacent to these cells no longer lie on the infection's perimeter; additionally, the remaining edges of this newly infected cell contribute at most 2 to this perimeter. All told, after infection, $P(A_1) \leq P(A_0)$.

If we suppose that $A_0$ is a lethal set, then at some point in time, the entire grid will become infected. This infection will have a perimeter $4n$. Since this perimeter did not increase, $A_0$ must have originally had a perimeter of at least $4n$. Since each cell in $A_0$ can contribute at most 4 to this perimeter, it must be the case that $|A_0| \geq n$. Our diagonal construction shows that $|A_0| \leq n$, and so we are able to conclude that $n$ is

best possible.

This proof is an instance of the famous *perimeter argument*, which has belonged to bootstrap percolation folklore since at least the work of Pete [8]. In the following section, we present generalizations of this argument to higher dimensional rectangular grids.

## 1.1 Bootstrap Percolation

The study of such cellular infection spread in grids (and, more generally, in graphs) is known in the literature as *bootstrap percolation*, and was introduced in the 1970s by Chalupa et al. [6] as a simplified model for the behavior of ferromagnetic fields. In their original 1979 paper, the authors research the stable structure of probabilistically selected initial infections. While this differs from the problem posed in Question 1, the rules for the spread of infection and its broad behavior remain the same. It is worth noting that a large portion of contemporary research on bootstrap problems is focused on questions of probabilistic nature; while these problems are certainly interesting and of merit, they do not fall within the scope of this thesis. Rather, we shall focus on those problems where we have specific control over the structure of the initial infections; in particular, we aim to determine the smallest lethal set on the Cartesian product of paths and cycles.

Let us now define the problem in concrete terms. Let $G$ be a graph, let $r \geq 0$ and let $A_0 \subseteq V(G)$ be a set of initially infected vertices. Iteratively, infect those vertices of $G$ with at least $r$ infected neighbors. For all $t > 0$, let $A_t$ be the set of infected vertices at time step $t$. We then have

$$A_t = A_{t-1} \cup \{v \in V(G) : |N_G(v) \cap A_{t-1}| \geq r\},$$

where $N_G(v)$ is the set of vertices adjacent to $v$ in $G$. We define the *closure* of $A_0$ under $r$-neighbor bootstrap percolation to be $[A_0] = \bigcup_{t=0}^{\infty} A_t$. We say that $A_0$ *percolates* or is *lethal* if $[A_0] = V(G)$. We define the smallest lethal set in a graph $G$ under $r$-neighbor bootstrap percolation by the quantity $m(G, r)$. We note that under these rules, it is not possible for vertices to become uninfected.

While it is possible to study bootstrap percolation on any graph $G$, much of the contemporary research focuses on multidimensional grids [**?**]. We therefore introduce the following notation. For all $n \in \mathbb{N}$, let $[n] = \{1, 2, \ldots, n\}$. Let the grid graph with vertex set $\prod_i^d [a_i]$ be denoted by $\prod_i^d [a_i]$. Note that $\prod_i^d [a_i] = P_{a_1} \square \cdots \square P_{a_d}$, where $\square$ denotes the Cartesian product of graphs. Furthermore, define:

$$m(a_1, \ldots, a_d, r) = m\left(\prod_i^d [a_i], r\right).$$

| $r$ | Grids | | | | | | | | |
|---|---|---|---|---|---|---|---|---|---|
| | $[a_1]$ | $[a_1] \times [a_2]$ | $[n]^2$ | $[a_1] \times [a_2] \times [a_3]$ | $[n]^3$ | $\cdots$ | $\prod_{i=1}^{d}[a_i]$ | $[n]^d$ | $[2]^d$ |
| $r=0$ | 0 | 0 | 0 | 0 | 0 | | 0 | 0 | 0 |
| $r=1$ | 1 | 1 | 1 | 1 | 1 | | 1 | 1 | 1 |
| $r=2$ | $\lceil \frac{a_1-1}{2} \rceil + 1$ | $\lceil \frac{a_1+a_2-2}{2} \rceil + 1$ | n | $\lceil \frac{a_1+a_2+a_3-3}{2} \rceil + 1$ | $\left\lceil \frac{3(n-1)}{2} \right\rceil + 1$ | | $\left\lceil \frac{\sum_{i=1}^{d}(a_i-1)}{2} \right\rceil + 1$ | $\left\lceil \frac{d(n-1)}{2} \right\rceil + 1$ | $\lceil \frac{d}{2} \rceil + 1$ |
| $r=3$ | **???** | **???** | $\lceil \frac{n^2+2n+4}{3} \rceil^*$ | **S.A. bound** | $n^2$ | | **???** | **???** | $\lceil \frac{d(d+3)}{6} \rceil$ |
| $\vdots$ | | | | | | $\ddots$ | | | |
| $r=d$ | **???** | **???** | **???** | **???** | **???** | | S.A. bound | $n^{d-1}$ | **???** |

Table 1.1: A summary of known bootstrap percolation results for grids and the torus, $r \in \{0, 1, 2, 3, d\}$.

There are a number of natural generalizations of the problem posed in Question 1. In this thesis, we discuss those obtained by varying the structure of $G$ and the value of $r$. Below, we outline some of the existing results for graphs that are the Cartesian product of paths and cycles, and $r \in \{0, 1, 2, 3\}$. These results are summarized in Table 1.1.

### 1.1.1 Results on grids and tori

In this section, we highlight existing extremal bootstrap percolation results on grids and tori. Some of the following bounds are not known to be tight and require supplemental constructions, which are often difficult to obtain. We further sub-divide this discussion into results on the grid (of which there are many), and results on the torus (of which there are few).

#### Grids

From the puzzle posed in Question 1, we readily obtain variant problems by altering three parameters: the size and shape of the grid $G$, the grid's dimension $d$, and the threshold number of neighbors $r$. We examine each of these problems in turn.

In the prior discussion of the perimeter argument, we showed that, for square grids, it holds that $m([n]^2, 2) \geq n$, and verified this to be tight with a diagonal construction. The following result (attributed to Pete) generalizes this result to all rectangular grids $[a_1] \times [a_2]$. A proof is included for completeness.

**Theorem 1.1.** *For $a_1, a_2 \geq 1$,*

$$m(a_1, a_2, 2) = \left\lceil \frac{a_1 + a_2}{2} \right\rceil.$$

*Proof.* We obtain a lower bound on $m(a_1, a_2, 2)$ by applying the perimeter argument. Note that the perimeter of the $a_1 \times a_2$ grid is $2(a_1+a_2)$, and so the $m(a_1, a_2, 2) \geq \left\lceil \frac{a_1+a_2}{2} \right\rceil$. (We take the ceiling because the size of infected sets must be integral. See Figure 1.4.)

Figure 1.3: Tight constructions for lethal sets where $a_1 + a_2 \leq 4$.

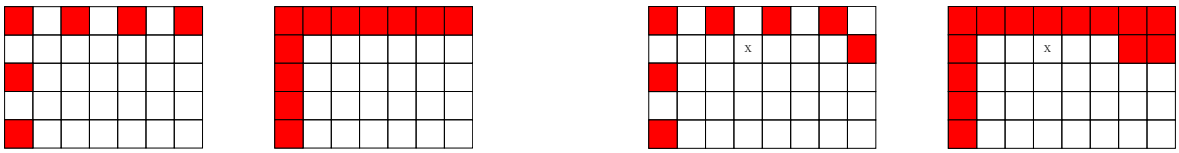


(a) $a + b \equiv 0 \pmod 2$ (b) $a + b \equiv 1 \pmod 2$

Figure 1.4: Tight constructions for lethal sets on the $[a] \times [b]$ grid.

For the upper bound, we proceed by induction on $a_1 + a_2$. For $a_1 + a_2 \leq 4$, the lethal sets in Figure 1.3 match the lower bounds given by the perimeter argument (1, 2, 2, and 2, respectively). For $a_1 + a_2 > 4$, suppose without loss of generality that $a_1 \leq a_2$, and so $a_2 \geq 3$. By hypothesis, $[a_1] \times [a_2 - 2]$ admits a lethal set $A_0$ at the perimeter bound. We show that $A_0$, plus the addition of any infection in the final column of $[a_1] \times [a_2]$, is lethal and matches the perimeter bound.

Observe that $A_0$ infects all vertices of $[a_1] \times [a_2]$, apart from the final two columns. The additional vertex in the final column is then sufficient to infect all remaining healthy vertices. Finally, by incrementing $a_2$ by two, the perimeter bound is incremented by exactly one. This completes the proof. □

Let us take a moment to examine the issue of integrality in the perimeter bound. When non-integrality occurs, either adjacent vertices are infected in the same generation, or a vertex is infected by more than $r$ neighbors. Note that in both cases, this decreases the perimeter of infection. One way to think about this is to consider each vertex as having "infectious potential": vertices $v \in A_0$ can infect up to $d(v)$ healthy vertices, whereas vertices $v \in A_i$ for $i > 0$ can infect at most $d(v) - r$. An integral perimeter bound mandates that each vertex realize its potential, whereas a non-integral bound leaves a small margin for error. Figure 1.4a illustrates the integral case, where each cell is infected by exactly two neighboring cells; this condition ensures that $P(A_i) = P([A_0])$ for all $i$. Conversely, in Figure 1.4b, the cell demarcated with an "X" experiences infection on three sides, thereby reducing its infectious potential. The existence of such a cell is guaranteed by the fact the perimeter bound in this case is non-integral.

We can further generalize in the case $r = 2$. In 2006, Balogh and Bollobás [1] proved the following general form of Theorem 1.1 for all $d$-dimensional hypercubes $(a_1, \ldots, a_d)$, $a_i \geq 1$:

**Theorem 1.2** (Balogh)**.** *For $d \geq 1$ and $a_1, \ldots, a_d \geq 1$,*

$$m(a_1, \ldots, a_d, 2) = \left\lceil \frac{\sum_{i=1}^{d}(a_i - 1)}{2} \right\rceil + 1.$$

Theorem 1.2 completes the picture for infections with a threshold of two on grids. The next question is whether similar results exist for larger $r$. Unfortunately, while generalizing to $d$-dimensional grids yields nice results for $r = 2$, attempts to obtain a holistic understanding of $m(a_1, \ldots, a_d, r)$ for arbitrary $r$ have been largely fruitless. Even the case of $r = 3$ remains stubbornly inaccessible for nearly all large $d$. However, certain breakthroughs have been made in the following circumstances: $d = 2$, $d = 3$, and $G = [2]^d$.

We first consider 3-neighbor percolation on two-dimensional square grids. In 2021, Benevides et al. proved that

$$m(n, n, 3) = \left\lceil \frac{n^2 + 2n + 4}{3} \right\rceil$$

for even $n$, and

$$\left\lceil \frac{n^2 + 2n}{3} \right\rceil \leq m(n, n, 3) \leq \left\lceil \frac{n^2 + 2n}{3} \right\rceil + 1$$

for odd $n$. Additionally, they showed that these bounds are tight for odd $n$: if $n = 5 \pmod 6$, or $n = 2^k - 1$ for some $k \in \mathbb{N}$, then $m(n, n, 3) = \lceil \frac{n^2+2n}{3} \rceil$; and if $n \in \{9, 13\}$, then $m(n, n, 3) = \lceil \frac{n^2+2n}{3} \rceil + 1$. Constructions that achieve this bound are illustrated in Chapter 7. We add to this picture with the following theorem, proven in Chapter 6, and corollary:

**Theorem 1.3.** *Suppose that $a, b \geq 1$ such that*

$$m(a, b, 3) = \frac{2ab + a + b}{3}.$$

*Then there exists $k \geq 1$ such that $a = b = 2^k - 1$.*

**Corollary 1.4.** *For all $n \geq 1$,*

$$m(n, n, 3) = \begin{cases} \left\lceil \frac{n^2+2n+4}{3} \right\rceil & n \equiv 0 \pmod 2 \\ \frac{n^2+2n}{3} & n = 2^k - 1,\ k \in \mathbb{N} \\ \frac{n^2+2n+1}{3} & n \equiv 5 \pmod 6 \\ \frac{n^2+2n+3}{3} & \textit{otherwise.} \end{cases}$$

*Proof.* The first three cases follow from Theorem 1 of [2] and the observation that if $n \equiv 5 \pmod 6$, then $\lceil \frac{n^2+2n}{3} \rceil = \frac{n^2+2n+1}{3}$. In the final case, $n$ is congruent to either 1 or

3 modulo 6. This implies that $n^2 + 2n$ is divisible by three. From Theorem 1 of [2], we have that $m(n, n, 3) \leq \frac{n^2+2n+3}{3}$. Furthermore, since $n$ is not of the form $2^k - 1$, it follows from Theorem 1.3 that $m(n, n, 3) > \frac{n^2+2n}{3}$. Therefore, $m(n, n, 3) = \frac{n^2+2n+3}{3}$. □

This result resolves the question of the minimum lethal set for two dimensional square grids. For the more general case of rectangular grids, the problem remains unsolved. However, we are able to achieve an upper bound of $m(a, b, 3) \leq \lceil \frac{ab+a+b+6}{3} \rceil$ and a lower bound (described below) of $m(a, b, 3) \geq \lceil \frac{ab+a+b}{3} \rceil$, for all $a, b > 1$. Further discussion of these results can be found in Chapter 6.

One significant and well-known result for 3-neighbor percolation on two- and three-dimensional grids is the following lower bound, taken as a three-dimensional analogue of the perimeter bound. This result is referenced frequently throughout this document, and referred to interchangeably as the *surface area* or *SA bound*. We prove the statement in full generality, while noting that we only make use of the case where $d = 3$. We also note that, like the perimeter bound, the following proof belongs to bootstrap percolation folklore, and appears to have been first published in 1997 by Balogh and Pete [**?**].

**Theorem 1.5.** *For any $d \geq 1$ and $a_1, a_2, \ldots, a_d \geq 1$,*

$$m(a_1, a_2, \ldots, a_d, d) \geq \frac{\sum_{j=1}^{d} \prod_{i \neq j} a_i}{d}.$$

*Proof.* We apply the same "invariant" strategy presented in the perimeter argument. For simplicity, consider $\prod_{i=1}^{d}[a_i]$ to be embedded within the larger graph $\prod_{i=1}^{d}\{0, \ldots, a_i + 1\}$. Note that in $\prod_{i=1}^{d}\{0, \ldots, a_i + 1\}$, each vertex $v \in \prod_{i=1}^{d}[a_i]$ has degree $2d$. Let $A_0$ be a lethal set in $\prod_{i=1}^{d}[a_i]$ under the $d$-neighbor bootstrap process. For $t > 0$, let $A_t$ be the set of infected vertices in $\prod_{i=1}^{d}[a_i]$ at generation $t$. Denote by $m_t$ the number of edges between vertices $u \in A_t$ and $v \in \prod_{i=1}^{d}[a_i] \setminus A_t$. We show that $m_{t-1} \geq m_t$ for all $t > 0$.

By definition, each vertex $v \in A_t \setminus A_{t-1}$ has at least $d$ neighbors in $A_{t-1}$. Therefore, since $d(v) = 2d$, $v$ has no more than $d$ neighbors outside of $A_t$. This implies that the number of edges from $A_{t-1} \cup \{v\}$ to $\prod_{i=1}^{d}[a_i] \setminus A_{t-1} \cup \{v\}$ cannot exceed $m_{t-1}$. Furthermore, this holds for every vertex $v \in A_{t-1}$, and so $m_{t-1} \geq m_t$.

Since $A_0$ is lethal, we have that

$$2d|A_0| \geq m_0 \geq m_1 \geq \cdots \geq 2\sum_{j=1}^{d} \prod_{i \neq j} a_i,$$

where the final expression gives the total number of edges between the fully infected grid and the surrounding larger grid. Dividing through by $2d$ gives the result. □

We note that the prior argument is precisely the same as the so-called perimeter argument outlined on Page 2. Here, the quantity $m_t$ is a $d$-dimensional analogue of the perimeter of infection $P(A_t)$ at time-step $t$, and the lower bound

$$2\sum_{j=1}^{d}\prod_{i\neq j}a_i$$

is the $d$-dimensional "perimeter" of the grid. Again, observe that equality can only be obtained when no vertices of $A_0$ are adjacent, and all vertices $v \in A_t$, for $t > 0$, are infected by exactly $d$ neighbors. Any imprecision causes a reduction in "perimeter" of two units, corresponding to a $1/d$ increase in the bound.

The primary aim of this thesis is to prove that the surface area bound is tight for sufficiently large grids when $r = 3$. This process employs a number of general constructions (discussed in Chapter 7), as well as a recursive strategy (Chapter 3). In Chapter 5, we prove the following result:

**Theorem 1.6.** *For all $a_1, a_2, a_3 \geq 11$,*

$$m(a_1, a_2, a_3, 3) = \left\lceil \frac{a_1a_2 + a_2a_3 + a_1a_3}{3} \right\rceil.$$

Unfortunately, the complete resolution of the $r = 3$ case on grids remains elusive. Tight constructions exist for cubes $[n]^3$ and hypercubes $[2]^d$, but in general bounds are difficult to obtain. Worse, for $r > 3$, the only additional result beyond the surface area bound addresses the very specific case of $r$-dimensional cubes. Open problems abound.

### Tori

In addition to varying the parameters $r$ and $d$, we might also change the very structure of $G$. It is natural to shift from grids (the Cartesian product of paths) to tori (the Cartesian product of cycles). In fact, it could be argued that bootstrap percolation on the torus is *more* natural than the grid, since tori are regular and grids are not. This problem has been studied by Benevides et al. In 2021, they obtained the following lower bound for the Cartesian product of two cycles [2]. Their proof is included here for completeness.

**Theorem 1.7.** *For $a, b \geq 1$,*

$$m(C_a \square C_b, 3) \geq \left\lceil \frac{ab+1}{3} \right\rceil.$$

*Proof.* Let $G = C_a \square C_b$, and let $I$ be a lethal set on $G$. Let $H = V(G) \setminus I$, and note that $|H| = ab - |I|$. Let $m_H$ be the number of edges in the subgraph of $G$ induced

by $H$, and $m_{IH}$ be the number of edges between vertices in $I$ and vertices in $H$. Note that $m_{IH}$ is similar to the notion of perimeter on a grid.

Observe that $G[H]$ must be cycle-free: cycles in $G[H]$ constitute immune regions, and contradict the lethality of $I$. Therefore, $G[H]$ is a forest, and so $m_H = |H| - c$, where $c$ is the number of components in $G[H]$. Additionally, note that $m_{IH} \leq 4|I|$, since $G$ is 4-regular. Finally, observe that the total degree of $G[H]$ is $2m_H = 4|H| - m_{IH}$.

Chaining together these inequalities, we obtain:

$$\begin{aligned} 4|I| \geq m_{IH} &= 4|H| - 2m_H \\ &= 4|H| - 2(|H| - c) = 2|H| + 2c \\ &= 2(ab - |I|) + 2c \end{aligned}$$

Combining like terms and simplifying, we have

$$|I| \geq \frac{ab + c}{3} \geq \frac{ab + 1}{3}.$$

□

Observe that the conditions $c \geq 1$ and $m_{IH} \leq 4|I|$ prevent us from obtaining strict equality. Specifically, if $I$ is lethal, $G[H]$ has one component, and no vertices in $I$ are adjacent, then $|I|$ is minimized. Note that these conditions are quite similar to those on grids; the specific difference is that equality in the bound on grids mandates that no vertex be infected by more than $r$ neighbors, whereas equality on three-dimensional tori requires this inefficiency be centered on one particular vertex.

Theorem 1.7 is generalized to all tori by Hambardzumyan, Hatami and Qian in [7]. Specifically, they provide a recursive formula for the size of minimum lethal sets on tori under $r$-bond bootstrap percolation, an instance of graph bootstrap percolation introduced by Bollobas in 1968 [5]. One might think of this process as an analogue of bootstrap percolation on the edges of a graph, whereby an uninfected edge becomes infected if one of its endpoints is adjacent to at least $r$ infected edges. The minimum lethal edge set under the $r$-bond process on a graph $G$ is denoted by $m_e(G, r)$.

The authors note that a lethal set of vertices can be converted into a lethal set of edges under the $r$-bond process by simply infecting an arbitrary set of $r$ edges incident to every infected vertex. This observation provides the following lower bound on $m(G, r)$:

$$\frac{m_e(G, r)}{r} \leq m(G, r).$$

In Theorem 8 of [7], a recursive formula is given for $m_e(G_d, r)$, where $G_d$ is the Cartesian product of $d$ cycles. As $m_e(G_d, r) = r \cdot m(G, r)$, we are able to leverage this result to obtain a lower bound on $m(C_{a_1} \square C_{a_2} \square C_{a_3}, 3)$. In particular, we have the following theorem.

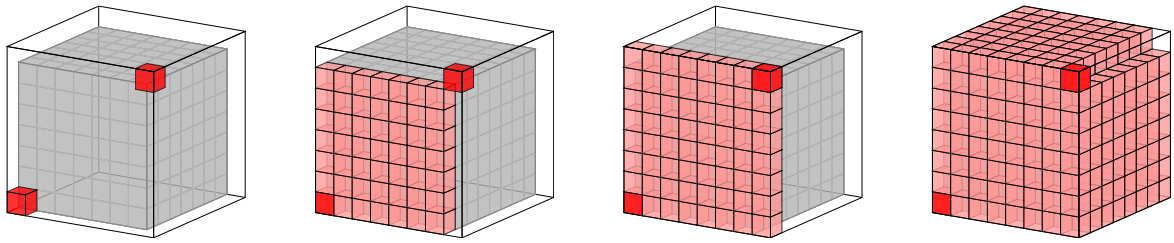

(a) (b) (c) (d)

Figure 1.5: Four stages of infection on the grid $G$ (gray) inset in the larger torus, with infected vertices $u$ and $v$ (dark red).

**Theorem 1.8.** *Let* $G_3 = C_{a_1} \square C_{a_2} \square C_{a_3}$. *Then*

$$m(G_3, 3) \geq \frac{(a_1-1)(a_2-1) + (a_2-1)(a_3-1) + (a_3-1)(a_1-1) + 3}{3}.$$

Note that the above bound is precisely one less than the surface area bound on the grid $[a_1 - 1] \times [a_2 - 1] \times [a_3 - 1]$. The following corollary to Theorem 1.6 provides an upper bound on $m(G_3, 3)$ for all $a_1, a_2, a_3 \geq 12$:

**Corollary 1.9.** *Let* $G_3 = C_{a_1} \square C_{a_2} \square C_{a_3}$, *where* $a_1, a_2, a_3 \geq 12$. *Then*

$$m(G_3, 3) \leq \frac{(a_1-1)(a_2-1) + (a_2-1)(a_3-1) + (a_3-1)(a_1-1) + 6}{3}.$$

*Proof.* Let $G = [a_1 - 1] \times [a_2 - 1] \times [a_3 - 1]$ and observe that, by Theorem 1.6,

$$\frac{(a_1-1)(a_2-1) + (a_2-1)(a_3-1) + (a_3-1)(a_1-1) + 6}{3} = SA(G, 3) + 2.$$

Consider $[a_1 - 1] \times [a_2 - 1] \times [a_3 - 1] \subset V(G_3)$, and let $A_0$ be a perfect lethal set on the grid induced by these vertices. Let $u = (a_1, a_2, a_3)$ and $v = (a_1, 1, 1)$ be vertices in $G_3$ (see Figure 1.5). We show that $A_0 \cup \{u, v\}$ is lethal on $G_3$.

Note that $A_0$ infects all vertices $[a_1 - 1] \times [a_2 - 1] \times [a_3 - 1]$. Consider $[a_1] \times [a_2 - 1] \times [a_3 - 1]$, and observe that the infection spreads outward across this face from $v$ (Figure 1.5b). With all of $a_1 \times [a_2 - 1] \times [a_3 - 1]$ infected, $u$ spawns infections down $a_1 \times a_2 \times [a_3 - 1]$ and $a_1 \times [a_2 - 1] \times a_3$ (Figure 1.5c). This permits infection of faces $[a_1 - 1] \times [a_2] \times [a_3 - 1]$ and $[a_1 - 1] \times [a_2 - 1] \times [a_3]$ (Figure 1.5d). Finally, $[a_1 - 1] \times a_2 \times a_3$ are infected (not pictured).

This constitutes all vertices of $G_3$, and so we conclude that $A_0 \cup \{u, v\}$ is lethal on $G_3$. □

### 1.1.2 Other Problems

Thus far, we have focused on the extremal problem of determining the smallest possible lethal set on $d$-dimensional grids and tori. Unsurprisingly, this is one of many existing areas of research in bootstrap percolation. In this section, we shall highlight a different, related problem: what is is the maximum (and minimum) time it takes for a lethal set to infect all vertices of a grid?

As before, we shall begin with 2-neighbor percolation on $[n]^2$, and address the question of maximum percolation time. We shall say that a lethal set $A_0 \subseteq V(G)$ percolates in time $T$ if we obtain $[A_0]$ in $T$ time-steps. For $r \in \mathbb{N}$, let

$$T(G, r) = \max\{T \in \mathbb{N} \mid \exists \text{ a set } A_0 \subseteq V(G) \text{ that } r\text{-neighbor percolates in time } T\}.$$

In 2015, Benevides and Przykucki [4] determined the asymptotic value of $T([n]^2, 2)$. Their result is reproduced below.

**Theorem 1.10** (Benevides, Przykucki)**.** *The maximum percolation time on* $[n]^2$ *is* $T([n]^2, 2) = \frac{13}{18}n^2 + O(n)$.

Interestingly, this time is not achieved with minimum lethal sets (of size $n$). In fact, the same authors showed in an earlier paper that the maximum percolation time for lethal sets $A_0$ on $[n]^2$, where $|A_0| = n$, is the nearest integer value to $\frac{5n^2-2n}{8}$ [3].

The fact that minimum lethal sets do not always percolate slowest holds for grids $[n]^2$ under 3-neighbor percolation, where $n = 2^k - 1$. In Chapter 5, we prove that $m([n]^2, 3) = \frac{n^2+2n}{3}$, and this is achieved for exactly one lethal configuration of vertices $A_0$. It is easy to see that $A_0$ percolates in time $(n-1)/2$ and so, if $|A_0| = \frac{n^2+2n}{3}$, then $T([n]^2, 3) = \frac{n-1}{2}$ (see Figure 1.6a). By removing the restriction on $|A_0|$, we are able to improve this to $T([n]^2, 3) \geq (n-1)(n-1)/2$ (see Figure 1.6b). It is not clear whether this lower bound is best possible and, as far as we are aware, no papers have been published regarding the value of $T([n]^d, r)$ for values other than $d = r = 2$.

## 1.2 Structure of this Thesis

As stated by Theorem 1.6, the primary goal of this thesis is to prove a tight bound for 3-neighbor bootstrap percolation on three-dimensional grids of sufficiently large size. This task requires the use of two major lemmas, as well as both original and previously published ideas and constructions. In an effort to present this material in a coherent manner, the thesis is structured as follows.

Chapters 2 and 3 are dedicated to building a conceptual and intuitive framework upon which to prove Theorem 1.6. In Chapter 2, we present lemmas regarding the structure of lethal sets in both two-dimensional and $d$-dimensional grids. These lemmas

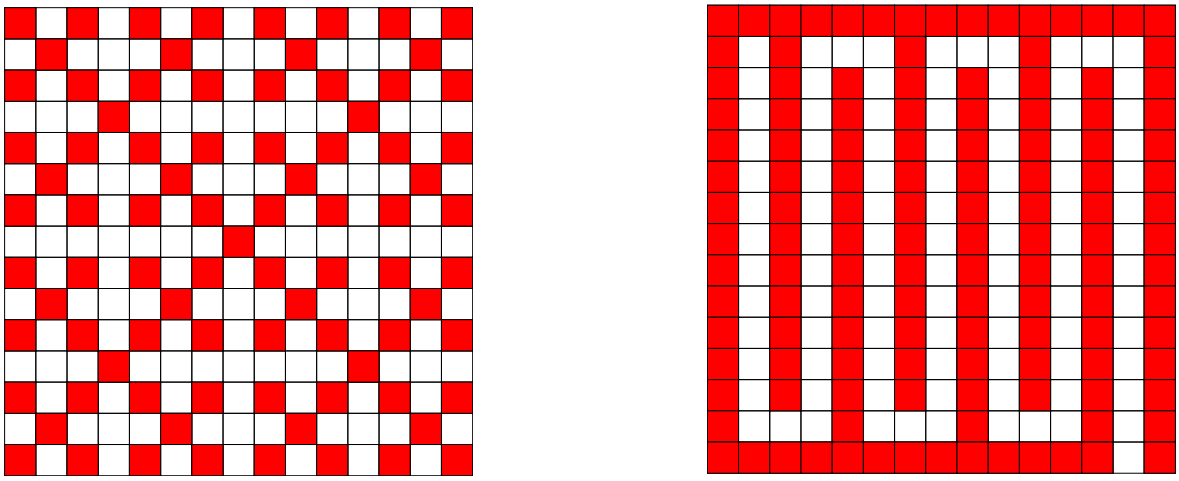

(a) $T([n]^2, 3) = \frac{n-1}{2}$ (b) $T([n]^2, 3) \geq \frac{(n-1)(n-1)}{2}$

Figure 1.6: Lethal sets on $[2^k - 1]^2$ with different percolation times.

will prove useful in our examination of general constructions of lethal sets (see Chapter 6). We also discuss the design and function of a visualization tool developed to assist in the examination of lethal sets. In Chapter 3, we prove a lemma that will allow us to recursively develop large families of lethal sets that match the surface area bound, and summarize all families of lethal sets that we are able to obtain.

Chapter 4 leverages the results of Chapters 2 and 3 to prove Theorem 1.6. We first show that all divisible grids $(a_1, a_2, a_3)$, $a_1 \leq a_2 \leq a_3$ admit lethal sets matching the SA bound, and then extend this result to all grids of size 11. Chapter 5 further builds on this, highlighting some new results for 3-neighbor percolation on grids of the form $(a_1, a_2, 1)$.

Chapter 7 and Appendix A examine the structure and lethality of percolating sets discovered in this research. In particular, Chapter 7 proves the lethality of the constructed families of sets presented in Chapter 2, and Appendix A illustrates the phases of infection on individual lethal sets.

Finally, Chapter 9 summarizes our results and provides recommendations for future research in similar and related problems.

# Chapter 2
# Tools and Techniques

As suggested in Chapter 1, it appears that lethal sets in grid graphs adhere to certain fixed rules. We examine these rules here, and explain why they are necessary and helpful for understanding the problem of bootstrap percolation.

## 2.1 The $d$-walls lemma

While it is difficult to identify specific patterns across all lethal sets $A_0$ under the $r$-neighbor bootstrap process, there are certain structures that appear frequently enough to warrant discussion. Of particular utility is the following lemma, which states precisely what it means for a set to span a grid (as we saw in Figure 1.2).

**Lemma 2.1.** *Let $A_0$ be an infected set on $G = \prod_{i=1}^{d}[a_i]$. Let $\overline{A_0} = V(G) \setminus A_0$, and let $H = G[\overline{A_0}]$ be the subgraph of $G$ induced by $\overline{A_0}$. For $1 \leq k \leq a_j$, let $F_{j,k} = \prod_{i=1}^{j-1}[a_i] \times \{k\} \times \prod_{i=j+1}^{d}[a_i]$ be the $k$th level of $G$ in the $j$th dimension. If $H$ does not contain a path between $F_{j,1}$ and $F_{j,a_j}$, for all $1 \leq j \leq d$, then $A_0$ is lethal on $G$ under $d$-neighbor percolation.*

*Proof.* We proceed by induction on $|V(H)| = \prod_{i=1}^{d} a_i - |A_0|$. If $|V(H)| = 0$, then all vertices of $G$ are infected and we are done. Suppose $|V(H)| > 0$, and consider a connected component $Y$ of $H$. By hypothesis, for all $j \in [d]$, either $V(Y) \cap F_{j,1} = \emptyset$ or $V(Y) \cap F_{j,a_j} = \emptyset$ (or both). Suppose, without loss of generality, that $V(Y) \cap F_{j,a_j} = \emptyset$. For each $j \in [d]$, let $x_j$ be the maximum value such that $V(Y) \cap F_{j,x_j}$ is non-empty. Note that such an $x_j$ must exist since $|V(H)| > 0$.

Consider the vertex $\vec{x} = (x_1, \ldots, x_d) \in V(Y)$, and observe that

$$\{\bigcup_{j\in[d]} F_{j,x_j+1}\} \cap V(Y) = \emptyset.$$

In particular, note that $(x_1 + 1, x_2, \ldots, x_d), \ldots, (x_1, \ldots, x_d + 1) \in N_S(\vec{x})$. Therefore, $\vec{x}$ becomes infected. Furthermore, since $|V(H) \setminus \{\vec{x}\}| < |V(H)|$, the resulting graph percolates by induction. This completes the proof. □

**Corollary 2.2.** *Let $G$ be the grid graph $\prod_{i=1}^{d}[a_i]$. For each $j \in [d]$ and some $1 \leq k \leq a_j$, let*

$$M = \bigcup_{j,k} F_{j,k}$$

*be a subset of the vertices of $G$ formed by the union of mutually orthogonal faces. If a set $A_0$ is lethal on $M$, then it is lethal on $G$.*

*Proof.* Since $A_0$ is lethal on $M$, there exists a time $t$ where $M \subseteq A_t$. Therefore, for all $j \in [d]$, the graph $G[\overline{A_t}]$ cannot contain a path between $F_{j,1}$ and $F_{j,a_j}$. By Lemma 2.1, $A_0$ is lethal on $G$. □

Corollary 2.2 provides a general description of lethal sets on $d$-dimensional grids in terms of their $(d-1)$-dimensional faces, provided these faces are mutually orthogonal. Here, we return to the notion first introduced in Chapter 1 of the capacity of a lethal set to span a grid. In particular, we see that the set in Figure 1.2a is comprised of lethal sets under the 2-neighbor bootstrap process on the two one-dimensional orthogonal faces $F_{1,1}$ and $F_{2,1}$ of $[10]^2$. In this regard, the problem of obtaining perfect $d$-neighbor lethal sets on $d$-dimensional grids is reduced to the problem of determining a "good" union $M$ of mutually orthogonal $(d-1)$-dimensional faces. In Chapter 7, we apply this idea to obtain an infinite family of three-dimensional grids from three orthogonal two-dimensional faces. However, we caution that the challenge of determining a "good" union $M$ is non-trivial in general.

The following corollary (taken as a particular instance of Corollary 2.2) will be useful in our discussion of lethal sets on three-dimensional grids $(a_1, a_2, a_3)$.

**Corollary 2.3.** *Let $G$ be the grid graph $(a_1, a_2, a_3)$. If a set $A_0$ is lethal on $F_{1,1} \cup F_{2,1} \cup F_{3,1}$, then $A_0$ is lethal on $G$.*

*Proof.* By hypothesis, $A_0$ is lethal on $F_{1,1} \cup F_{2,1} \cup F_{3,1}$. Therefore, there exists some time $t$ for which $F_{1,1} \cup F_{2,1} \cup F_{3,1} \subseteq A_t$, and so $G[\overline{A_t}]$ satisfies the conditions of Lemma 2.1. We conclude that $A_0$ is lethal on $G$. □

In the case of three-dimensional grids, it is instructive to think of the perpendicular faces $M = F_{1,1} \cup F_{2,1} \cup F_{3,1}$ as an unfolded surface (see Figure 2.1). We refer to $M$ as a manifold of $G$, and to this unfolded surface as a *proper unfolding* of $M$. In Chapter 7, we examine other manifolds and their proper unfoldings.

Since, by Corollary 2.2, any lethal set on $M$ is also lethal on $G$, it is often easier to identify lethal sets by examining these flattened unfolded structures. In fact, in the particular case of $M = F_{1,1} \cup F_{2,1} \cup F_{3,1}$, the surface area bound on $(a_1, a_2, a_3)$ can be written in terms of the surface area bounds on flat, two-dimensional grids.

**Lemma 2.4.** *For $a_1 \geq a_2 \geq a_3 \geq 1$,*

$$SA(a_1, a_2, a_3) = SA(a_1 + a_3 - 1, a_2 + a_3 - 1, 1) - SA(a_3 - 1, a_3 - 1, 1).$$

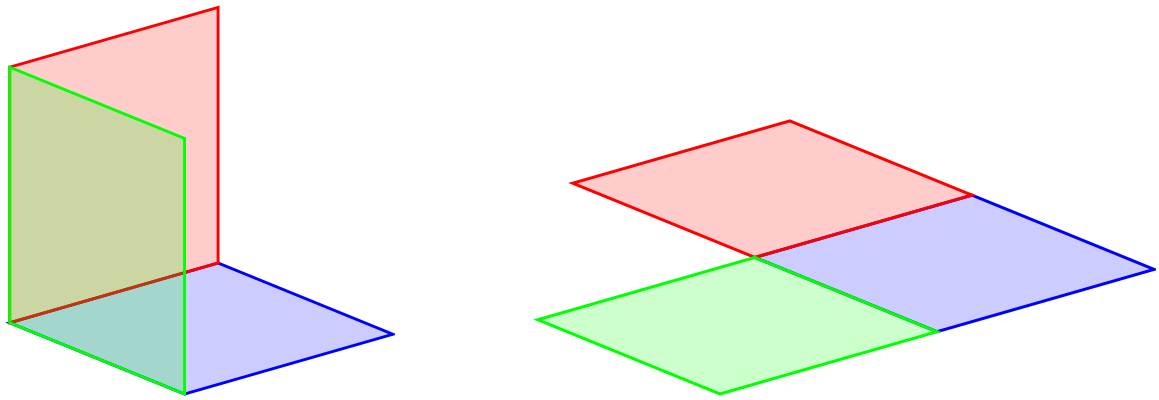

Figure 2.1: Three perpendicular faces of $(a_1, a_2, a_3)$ (left) and their representation as a flat unfolded surface (right).

*Proof.* Taking the surface area bound on the righthand side of the above equation, we obtain

$$\mathrm{SA}(a_1 + a_3 - 1, a_2 + a_3 - 1, 1) = \frac{a_1a_2 + a_1a_3 + a_2a_3 + a_3^2 - 1}{3}$$

and

$$\mathrm{SA}(a_3 - 1, a_3 - 1, 1) = \frac{a_3^2 - 1}{3}.$$

Adding these two expressions together gives

$$\frac{a_1a_2 + a_1a_3 + a_2a_3}{3},$$

which is precisely the surface area bound for $(a_1, a_2, a_3)$. □

In the context of Figure 2.1, this lemma tells us that a percolating set on the $(a_1, a_2, a_3)$ grid (left of Figure 2.1) is precisely the same size as a percolating set on the complete flattened rectangle minus the size of a percolating set on the missing region (right of Figure 2.1). In practice, this lemma allows us to leverage an understanding of lethal sets on two-dimensional grids to obtain lethal sets in three dimensions. However, care is required in this process, and the existence of an optimal set on a two-dimensional grid does not immediately guarantee the existence of such a set in three dimensions.

## 2.2 3-neighbor percolation on two-dimensional grids

It is clear that an understanding of the behavior of 3-neighbor percolation on two-dimensional grids is of use in our investigation of 3-neighbor percolation on $(a_1, a_2, a_3)$ grids. In Chapter 6 we examine the problem of 3-neighbor percolation on square two-dimensional grids, and answer a question posed by Benevides et alia regarding the value

| mod 3 | $a_1 \equiv 0$ | $a_1 \equiv 1$ | $a_1 \equiv 2$ |
|---|---|---|---|
| $a_2 \equiv 0$ | | | |
| $a_2 \equiv 1$ | | | |
| $a_2 \equiv 2$ | | | |

(a) $a_3 \equiv 1 \pmod 3$

| mod 3 | $a_1 \equiv 0$ | $a_1 \equiv 1$ | $a_1 \equiv 2$ |
|---|---|---|---|
| $a_2 \equiv 0$ | | | |
| $a_2 \equiv 1$ | | | |
| $a_2 \equiv 2$ | | | |

(b) $a_3 \equiv 2 \pmod 3$

| mod 3 | $a_1 \equiv 0$ | $a_1 \equiv 1$ | $a_1 \equiv 2$ |
|---|---|---|---|
| $a_2 \equiv 0$ | | | |
| $a_2 \equiv 1$ | | | |
| $a_2 \equiv 2$ | | | |

(c) $a_3 \equiv 0 \pmod 3$

Table 2.1: Integrality of grids by congruence class. Green indicates integral surface area bound.

of $m([n]^2, 3)$. Here, we describe some of the structural properties of lethal sets on two-dimensional grids that will prove useful in that analysis. The following propositions are due to Benevides et al [**?**].

**Proposition 2.5.** *Let $A_0$ be a lethal set on $[a_1] \times [a_2]$ under 3-neighbor percolation. Then $A_0$ contains all four corner vertices of $[a_1] \times [a_2]$.*

*Proof.* Since corner vertices in $[a_1] \times [a_2]$ have degree 2, they cannot become infected. Therefore, since $A_0$ is lethal, it must contain all corner vertices. □

**Proposition 2.6.** *Let $B$ be the set of vertices on the border of $[a_1] \times [a_2]$, and let $u, v \in B$ be adjacent vertices. If $A_0$ is a lethal set under 3-neighbor percolation, then $A_0 \cap \{u, v\} \neq \emptyset$.*

*Proof.* Assume for contradiction that $A_0 \cap \{u, v\} = \emptyset$. Since $u, v$ are border vertices, $d(u) \leq d(v) \leq 3$. Because $A_0$ is lethal, $u$ and$v$ must become infected. Suppose, without loss of generality, that $u$ is infected first. This is impossible, since $d(u) \leq 3$ and $v$ is not infected. □

**Proposition 2.7.** *Let $A_0$ be a lethal set on $[a_1] \times [a_2]$ under 3-neighbor percolation. Let $H = V([a_1] \times [a_2]) \setminus A_0$. Then the subgraph induced by $H$ is acyclic and each component of $H$ contains at most one border vertex.*

*Proof.* Suppose for contradiction that $C$ is a cycle in $H$. Let $v \in C$ be the first vertex of $C$ to become infected. Note that $v$ has two uninfected neighbors in $C$. Since $d(v) \leq 4$, $v$ cannot become infected, a contradiction.

Suppose $P$ is a path in $H$ with endpoints on the border. No vertex $v$ in $P$ can become infected, since $v$ has at most two neighbors outside of $P$. □

Proposition 2.7 more clearly articulates the notion of immune regions discussed in Chapter 1. While such immune regions exist in higher-dimensional grids, their structure is substantially harder to define.

It will be insightful to consider the surface area bound on two-dimensional grids in the context of Propositions 2.5, 2.6 and 2.7. For simplicity, we introduce the following terms. We refer to grids with integral surface area bounds as *divisibility cases* and

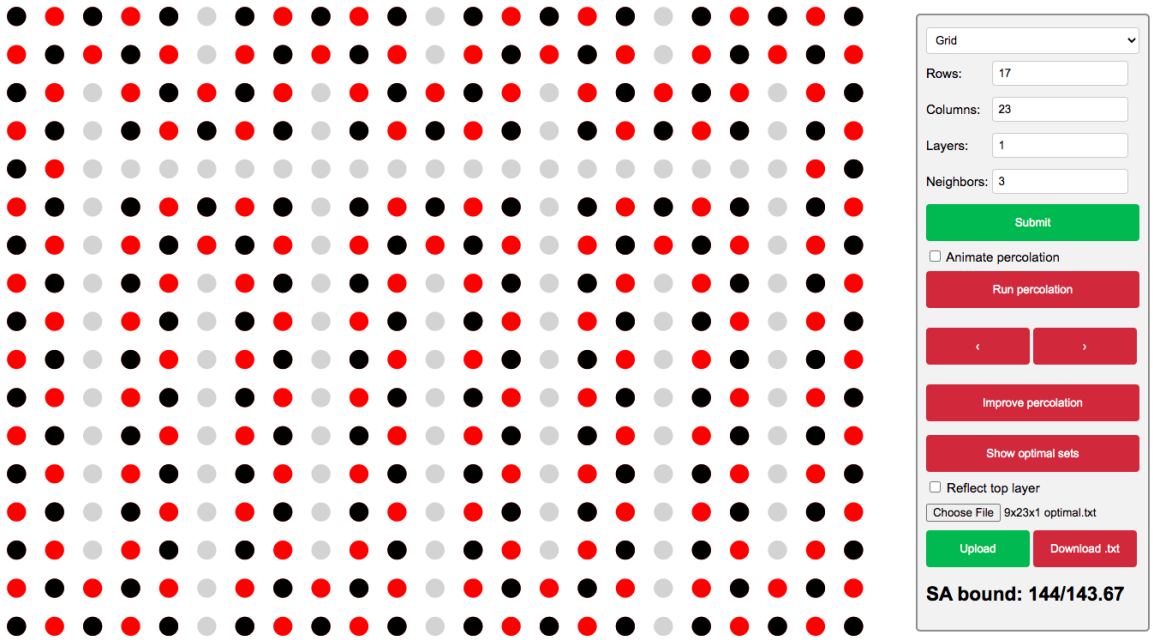


Figure 2.2: The visualization tool with a infected set.

grids with non-integral bounds as *non-divisibility cases*. The divisibility and non-divisibility cases for three-dimensional grids where $r = 3$ are illustrated in Table 2.1. Let $A_0 \subseteq V(G)$ be a lethal set on $G$ that matches the surface area bound. We call $A_0$ *perfect* if $G$ is a divisibility case, and *optimal* if $G$ is a non-divisibility case.

Recall from Chapter 1 that a lethal initial infection $A_0$ is perfect if it contains no adjacent vertices, and if all vertices $v \in A_{t>0}$ are infected by precisely $d$ neighbors. Therefore, by Propositions 2.5 and 2.6, if $[a_1] \times [a_2]$ admits a perfect lethal set, then $a_1, a_2 \equiv 1 \pmod 2$. Furthermore, every component of the subgraph $H$ induced by uninfected vertices must contain exactly one border vertex (otherwise the second condition on perfect infections would be violated). In Chapter 6, we use these observations to prove that the only two-dimensional grids that admit perfect lethal sets under 3-neighbor bootstrap percolation are of the form $[2^n - 1]^2$.

## 2.3 Visualizer

In addition to the conceptual tools presented above, many of the results in this thesis were obtained with the help of a visualization tool. This resource allows a user to experimentally infect vertices in two- and three-dimensional grids, and observe the step-by-step $r$-neighbor percolation process. As far as we are aware, such a tool did not previously exist for the problem of bootstrap percolation. In this section, we provide an overview of the functionality of this resource (which we refer to as the *visualizer*), and highlight features that could prove useful in further research. The visualizer is

located at `https://ahblay.pythonanywhere.com`, and the reader is encouraged to examine the lethal sets presented in later chapters as they appear (although this is not necessary to understand the results).

### 2.3.1 Control panel

The basic functionality of the visualizer allows a user to enter the parameters of their problem, select a set of initially infected vertices, and step through the percolation process by time-step. These options are made available to the user in a control panel, shown on the righthand side of Figure 2.2. The control panel features the following:

- A dropdown menu to choose between percolation on a grid, and percolation on a torus;
- Text boxes to enter the size of the grid (resp. torus);
- A text box to enter the threshold number of neighbors to spawn an infection;
- A submit button, which renders the chosen parameters as a grid of clickable gray circles;
- Buttons to initiate and step through the percolation process, and a checkbox to animate it;
- A button labeled "Improve percolation," which removes unnecessary infections (should they exist);
- An option to select from a list of existing lethal sets;
- A checkbox to reflect infected vertices;
- Buttons to upload/download an infected set as a text file.

We highlight the design and representation of grids as matrices of clickable vertices, the choice between grid and torus, the "Improve percolation" button, the ability to view existing lethal sets as well as upload/download them, and the option to reflect the pattern of infected vertices.

One of the challenges of visualizing the problem of bootstrap percolation arises from the fact that many grids are large and high-dimensional. This is perhaps the greatest limitation of the visualizer. The current iteration of the tool renders vertices as clickable regions in an HTML `canvas` element, which does not respond well to re-scaling. As a result, large grids contain very small vertices, which complicates the process of selecting an initial infection. Furthermore, `canvas` does not natively support 3-dimensional structures, and so 3-dimensional grids are simply rendered as a stack of their 2-dimensional layers.

Users are able to select between percolation on a grid, and percolation on a torus. This choice does not impact the representation of the grid (resp. torus). However, when stepping through the phases of infection, vertices at the top of the grid are treated as neighbors of those on the bottom, and similarly for left and right.

In this chapter (and in Chapter 6) we saw (shall see) that certain patterns of infected vertices are always lethal. The fickleness of bootstrap percolation regularly precludes us from simply copying these patterns across all grids to obtain perfect lethal sets. However, sometimes these patterns can be augmented with additional infections. If a set $A_0$ is lethal and above the surface area bound, the "Improve percolation" button attempts to remove non-essential infections. It does this by removing a random vertex $v$ from $A_0$ and checking if the resulting set is lethal. If it is, the new infection $A_0 \setminus \{v\}$ is rendered on the screen.

In pursuit of determining new perfect lethal sets, it is often helpful to examine and alter existing ones. Whenever a user clicks "Run percolation" on a perfect lethal set, a text file containing the lethal configuration of vertices is stored in a database. This file is made accessible to all future users through the "Show optimal sets" window. We hope that ongoing use of this tool will passively allow for the accumulation of a number of lethal sets in 2- and 3-dimensions. In addition to accessing known lethal sets via the "Show optimal sets" button, users are able to upload sets from a local text file. These files must be configured as a sequence of X's and O's, with rows on new lines, and layers separated by a blank line. An example of this format can be obtained by creating an infected grid on the visualizer and selecting "Download .txt".

The "Reflect top layer" checkbox is another resource designed to increase the efficiency of experimentally generating lethal sets. We have found in our research that certain grids, especially of the form $[a_1] \times [a_2] \times [2]$, have symmetric infections in their top and bottom layers. By choosing "Reflect top layer", these symmetries are generated automatically.

### 2.3.2 Design

### 2.3.3 Improvements

The visualization tool was developed primarily as a means to engage with the structure of lethal sets directly. Initially, it was intended as a private tool to help discern the often complex patterns in these sets. For this reason, it contains a number of quirks and bugs that were either treated as features, or ignored and never resolved. In this section, we discuss some of these issues and suggest possible improvements to make the tool useful to a broader audience.

The most significant bug occurs when a user attempts to alter an infected set during the percolation process. This bug is a direct consequence of the manner in which

As we discussed in the prior section, one limitation of HTML `canvas` elements is the inability to conveniently represent three dimensional objects. We circumvented this issue by representing grids as a sequence of two-dimensional layers. While this strategy is effective, it limits a user's ability to clearly identify patterns that appear between these layers. Through experimentation, we found that toggling between different orientations of the grid allowed us to discover patterns that were otherwise hidden. In the current version of the visualizer, there is no convenient way to obtain different orientations of a grid. We propose an additional button that cycles through the $d$ orientations of a grid. This feature would likely be simple to implement, and yield substantial results.

We also discussed the challenge of clicking on vertices in large grids, due to the inability to effectively zoom in on the `canvas` element. While the best solution to this problem likely requires a complete overhaul of the representation of the grid (using some other front-end library designed to better represent and interact with grid-like structures), an intermediate and simpler possibility is to improve the manner in which vertices are selected. In particular, we propose a change that allows sequences of vertices to be simultaneously selected by clicking and dragging. This should be fairly easy to implement, as one can track the `mouseDown` event in Javascript, and keep a list of the vertices that the cursor touches during this time.

When attempting to construct a lethal set, it is often the case that one begins with a particular configuration of vertices, and makes small changes to accommodate the particular parity or congruence class of the grid. One existing resource to aid in this process is the "Improve percolation" button. In its current state, this button is only able to remove unnecessary vertices from already lethal sets. However, it would we useful if it could also augment existing sets in such a way that they become more infectious. This could take the form of either adding vertices to infectious sets that are below the surface area bound, or changing the position of existing infections to increase the infectiousness of the initial set.

In a similar vein, recall that non-integral sets $A_0$ contain vertices that experience infection from more than $r$ neighbors. If the size of $A_0$ is well above the surface area bound, the location of such vertices can provide a good indication of where improvements in the structure of $A_0$ are likely to be found. One possible implementation could be to highlight vertices that do not realize their "infectious potential".

From a cosmetic perspective, the presentation of existing perfect lethal sets is currently difficult to parse and should be improved. We suggest that these files be arranged by the number of layers in the grid. Additionally, there is currently no capacity to represent and store constructions that apply to large families of grids. We currently provide large example files that clearly exhibit a repeating pattern. However, this choice is both less convenient and less convincing.

# Chapter 3
# A Recursive Technique

In the previous chapter, we examined some structures in grids that, if present, immediately guarantee lethality. Most significantly, we proved that lethal sets on mutually orthogonal walls of a grid are lethal on the entire grid. In the following sections, we leverage this result to show that certain configurations of fully infected sub-grids (which we shall call blocks) will cause the larger grid to become infected. Furthermore, we show that if each of these smaller blocks is infected with a minimum lethal set, the composite larger brick will also be infected with a minimum lethal set (barring some considerations for divisibility).

The proof of this claim makes use of the so-called *modified bootstrap process* in $[n]^d$, discussed in [**?**] and [**?**]. This is a strengthened variation of the problem introduced in Chapter 1, whereby vertices in the $[n]^d$ grid become infected if and only if they are adjacent to infected vertices along edges in each of the $d$ directions. For example, in the $[n]^2$ grid, a vertex that sees infection in one of both the North/South and East/West directions will itself become infected, whereas a vertex with infected neighbors to the East and West (but not North and South) will not.

In particular, the following lemma considers composite grids $[n]^d$ where each vertex $x = (x_1, \ldots, x_d) \in [n]^d$ is itself a smaller block $G_x$. We prove that lethal sets on these grids can be built from the smaller lethal sets on each $G_x$.

**Lemma 3.1.** *For $n, d \geq 1$, let $A = (a_{i,j})$ be a $d \times n$ matrix of positive integers, and let $b_i = \sum_{j=1}^{n} a_{i,j}$, for $1 \geq j \geq d$. Let $S$ be a lethal set under the modified process on $[n]^d$, and for each vertex $\vec{x} = (x_1, \ldots, x_v) \in S$, let $T_{\vec{x}}$ be a lethal set on $\prod_{i=1}^{d}[a_{i,x_i}]$ under $d$-neighbor percolation. Then*

$$m(b_1, \ldots, b_d, d) \leq \sum_{\vec{x} \in S} |T_{\vec{x}}|.$$

*Proof.* We imagine sub-dividing the $\prod_{i=1}^{d}[b_i]$ brick into smaller blocks by partitioning each of the $d$ axes into segments $a_{i,1}, a_{i,2}, \ldots, a_{i,n}$, $1 \leq i \leq d$. Each block is given by a unique product of these segments, and represented by a vector $\vec{x} = (x_1, \ldots, x_d) \in [n]^d$.

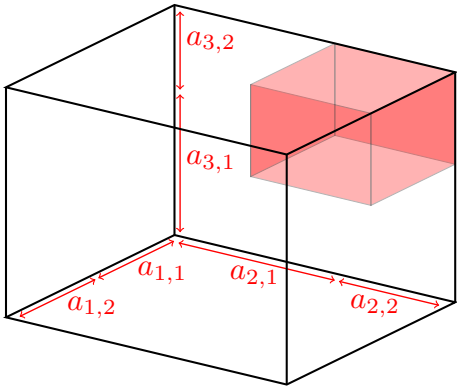


Figure 3.1: A recursively constructed $[b_1] \times [b_2] \times [b_3]$ grid, for $n = 2$, $d = 3$.

Formally, for each such $\vec{x}$, let $G_{\vec{x}}$ be the block with vertex set

$$\prod_{i=1}^{d} \{1 + \sum_{j=1}^{x_i - 1} a_{i,j}, \ldots, \sum_{j=1}^{x_i} a_{i,j}\},$$

and edges between vertices that differ by one in exactly one coordinate. Figure 3.1 illustrates the block $G_{\vec{x}}$ for $\vec{x} = (1, 2, 2) \in [2]^3$. Observe that $G_{\vec{x}}$ is isomorphic to $\prod_{i=1}^{d} [a_{i,x_i}]$.

For each $\vec{x} \in S$, let $A_{\vec{x}}$ be the vertices of $G_{\vec{x}}$ corresponding to the vertices of $T_{\vec{x}}$ under isomorphism from $\prod_{i=1}^{d} [a_{i,x_i}]$ to $G_{\vec{x}}$, and let $A_0 = \cup A_{\vec{x}}$. Observe that $|A_0| = \sum_{\vec{x} \in S} |T_{\vec{x}}|$. We show that $A_0$ is lethal on $\prod_{i=1}^{d} [b_i]$.

By the definition of $T_{\vec{x}}$, for each $\vec{x} \in S$, $A_{\vec{x}}$ is lethal on $G_{\vec{x}}$. Imagine running the $d$-neighbor process until all blocks $G_{\vec{x}}$ are fully infected. We claim that this is sufficient to infect all remaining vertices of $\prod_{i=1}^{d} [b_i]$. Consider the remaining blocks $G_{\vec{x}}$, for $\vec{x} \in [n]^d \setminus S$. Since $S$ is lethal under the modified process, each $G_{\vec{x}}$ is adjacent to fully infected blocks in all $d$ directions. In particular, if we consider expanding out the faces of $G_{\vec{x}}$ towards these infected blocks, the resulting cube has $d$ fully infected faces that share a common corner. By Corollary 2.3, this structure will infect all the vertices of $G_{\vec{x}}$. Repeating this process on each uninfected region of $\prod_{i=1}^{d} [b_i]$ (as they are exposed under the modified process) ultimately results in all vertices becoming infected. This completes the proof. □

We note that although the lemma above is true in full generality, we are only concerned with the particular case where $n = 2$ and $d = 3$. The following corollary proves that the bound in Lemma 3.1 is tight for $n = 2$ and $d = 3$, if lethal sets on at least three of the constituent blocks are perfect.

**Corollary 3.2.** *Let $A = (a_{i,j})$ be a $3 \times 2$ matrix of positive integers, and let $b_i = a_{i,1} + a_{i,2}$*

*for all* $1 \leq i \leq 3$. *Then* $m(b_1, b_2, b_3, 3)$ *is at most*

$$m(a_{1,1}, a_{2,1}, a_{3,1}, 3) + m(a_{1,2}, a_{2,2}, a_{3,1}, 3) + m(a_{1,2}, a_{2,1}, a_{3,2}, 3) + m(a_{1,1}, a_{2,2}, a_{3,2}, 3).$$

*Furthermore, this bound is tight if at least 3 of the constituent grids are perfect.*

*Proof.* The upper bound on $m(b_1, b_2, b_3, 3)$ is a direct consequence of Lemma 3.1, since $(1,1,1), (2,2,1), (2,1,2), (1,2,2)$ is lethal under the modified process on $[2]^3$.

If all grids are perfect, then:

$$\begin{aligned}
&m(a_{1,1}, a_{2,1}, a_{3,1}, 3) + m(a_{1,2}, a_{2,2}, a_{3,1}, 3) + m(a_{1,2}, a_{2,1}, a_{3,2}, 3) + m(a_{1,1}, a_{2,2}, a_{3,2}, 3) \\
&= \frac{a_{1,1}a_{2,1} + a_{2,1}a_{3,1} + a_{3,1}a_{1,1}}{3} + \frac{a_{1,2}a_{2,2} + a_{2,2}a_{3,1} + a_{3,1}a_{1,2}}{3} \\
&\qquad + \frac{a_{1,2}a_{2,1} + a_{2,1}a_{3,2} + a_{3,2}a_{2,1}}{3} + \frac{a_{1,1}a_{2,2} + a_{2,2}a_{3,2} + a_{3,2}a_{1,1}}{3} \\
&= \frac{(a_{1,1} + a_{1,2})(a_{2,1} + a_{2,2}) + (a_{2,1} + a_{2,2})(a_{3,1} + a_{3,2}) + (a_{3,1} + a_{3,2})(a_{1,1} + a_{1,2})}{3} \\
&= \frac{b_1b_2 + b_2b_3 + b_3b_1}{3}.
\end{aligned}$$

Similarly, suppose, without loss of generality, that $(a_{1,1}, a_{2,1}, a_{3,1})$ is optimal and the remaining grids are perfect. Then:

$$\begin{aligned}
&m(a_{1,1}, a_{2,1}, a_{3,1}, 3) + m(a_{1,2}, a_{2,2}, a_{3,1}, 3) + m(a_{1,2}, a_{2,1}, a_{3,2}, 3) + m(a_{1,1}, a_{2,2}, a_{3,2}, 3) \\
&= \left\lceil \frac{a_{1,1}a_{2,1} + a_{2,1}a_{3,1} + a_{3,1}a_{1,1}}{3} \right\rceil + \frac{a_{1,2}a_{2,2} + a_{2,2}a_{3,1} + a_{3,1}a_{1,2}}{3} \\
&\qquad + \frac{a_{1,2}a_{2,1} + a_{2,1}a_{3,2} + a_{3,2}a_{2,1}}{3} + \frac{a_{1,1}a_{2,2} + a_{2,2}a_{3,2} + a_{3,2}a_{1,1}}{3} \\
&= \left\lceil \frac{(a_{1,1} + a_{1,2})(a_{2,1} + a_{2,2}) + (a_{2,1} + a_{2,2})(a_{3,1} + a_{3,2}) + (a_{3,1} + a_{3,2})(a_{1,1} + a_{1,2})}{3} \right\rceil \\
&= \left\lceil \frac{b_1b_2 + b_2b_3 + b_3b_1}{3} \right\rceil.
\end{aligned}$$

In both cases, we obtain the lower bound $m(b_1, b_2, b_3, 3)$. This completes the proof. □

## 3.1 Applying the recursion

Corollary 3.2 provides a prescriptive method for constructing optimal and perfect lethal sets recursively, provided the existence of sufficiently many small building blocks. In

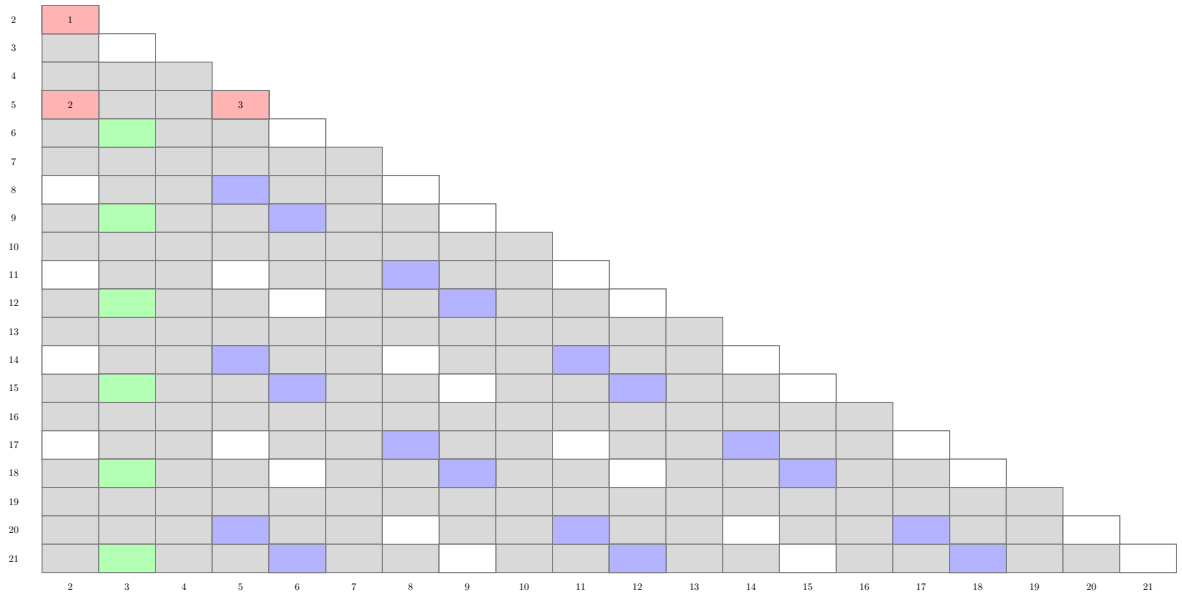


Table 3.1: Thickness 2 constructions used in the proof of Theorem 1.6. Blue and green cells represent infinite families of constructions. Red cells are individual constructions. Divisibility cases are white and non-divisibility cases are gray.

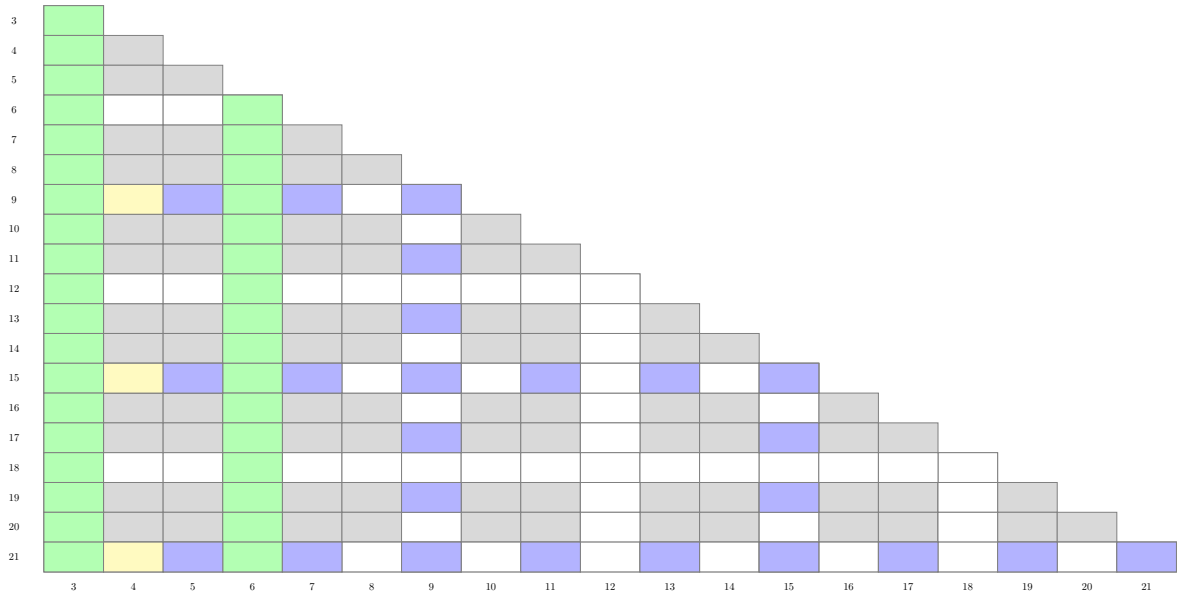


Table 3.2: Thickness 3 constructions used in the proof of Theorem 1.6. Blue, green and yellow cells represent infinite families of constructions. Red cells are individual constructions. Divisibility cases are white and non-divisibility cases are gray.

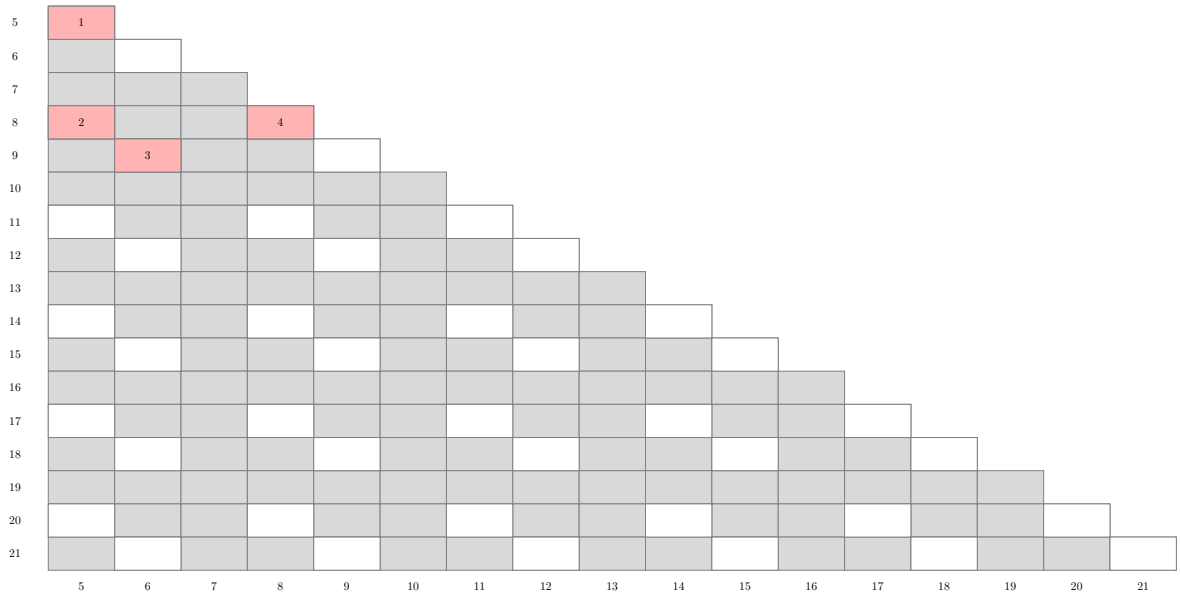


Table 3.3: Thickness 5 constructions used in the proof of Theorem 1.6. Red cells are individual constructions. Divisibility cases are white and non-divisibility cases are gray.

the following chapter, we use this technique to obtain perfect lethal sets on all $(b_1, b_2, b_3)$ grids, for $b_1, b_2, b_3 \geq 5$, and optimal lethal sets on all $(b_1, b_2, b_3)$ grids, for $b_1, b_2, b_3 \geq 11$. To facilitate this process, we first summarize some useful families of lethal sets (discussed in greater detail in Chapter [Constructions] and illustrated in Tables 3.1, 3.2, and 3.3), as well as particular applications of Corollary 3.2 that hold for general grids.

**Proposition 3.3.** *For all $k \geq 1$ such that $k \neq 2$, $(3, 3, k)$ is perfect.*

*Outline.* We obtain $(3, 3, k)$ for $k \equiv 0 \pmod 2$ and $k > 2$ from Construction 6.8, and $(3, 3, k)$ for $k \equiv 1 \pmod 2$ and $k > 2$ from Construction 6.9. The case of $(3, 3, 1)$ is given in Benevides, and reproduced as Construction 5.7. □

**Proposition 3.4.** *For all $k \geq 2$, $(3, 6, k)$ is perfect.*

*Outline.* WE NEED THIS CONSTRUCTION TO BE WRITTEN UP. □

**Proposition 3.5.** *For all $k \equiv 3 \pmod 6$ and $l \equiv 1 \pmod 2$ such that $l > 1$, $(3, k, l)$ is perfect.*

*Outline.* We obtain such grids from Construction 6.9. □

**Proposition 3.6.** *For all $k, l \in \{0, 2, 3, 5\} \pmod 6$ such that $k \not\equiv l \pmod 6$ and $k, l > 2$, $(k, l, 2)$ is perfect.*

*Outline.* We obtain $(k, l, 2)$ for $k, l \in \{2, 5\} \pmod 6$ such that $k \not\equiv l \pmod 6$ and $k, l > 2$ from Construction 6.6. We obtain $(k, l, 2)$ for $k, l \in \{0, 3\} \pmod 6$ such that $k \not\equiv l \pmod 6$ and $k, l \geq 6$ from Construction 6.7. The remaining grids are of the form $(k, 3, 2)$ for $k \equiv 0 \pmod 6$ and these are obtained from Construction 6.5. □

**Proposition 3.7.** *For all $k \equiv 3 \pmod 6$, $(k, 4, 3)$ is perfect.*

*Outline.* We obtain $(k, 4, 3)$ for $k \equiv 3 \pmod 6$ and $k \geq 9$ from Construction 6.10. The case of $(4, 3, 3)$ is given by Proposition 3.3. □

**Proposition 3.8.** *For all $k \equiv 0 \pmod 6$ such that $k > 3$, $(k, 2, 3)$ is perfect.*

*Outline.* We obtain $(k, 2, 3)$ for $k \equiv 0 \pmod 6$ and $k \geq 6$ from Construction 6.5. □

**Proposition 3.9.** *For all $k \equiv 3 \pmod 6$ such that $k > 3$, $(k, 2, 3)$ is perfect.*

*Outline.* We obtain $(k, 2, 3)$ for $k \equiv 3 \pmod 6$ and $k > 3$ from Construction 6.4. □

**Proposition 3.10.** *For all $k \geq 1$, $(2^k - 1, 2^k - 1, 1)$ is perfect.*

*Outline.* The construction for such grids is presented in Benevides and reproduced as Construction 5.7. □

Combining the above propositions with Corollary 3.2, we are able to obtain the following lemmas.

**Lemma 3.11.** *Suppose $(b_1, b_2, b_3)$ is optimal. Then $(b_1 + 3, b_2 + 3, b_3 + 3)$ is optimal.*

*Proof.* By Proposition 3.3, each of $(b_1, 3, 3), (3, b_2, 3), (3, 3, b_3)$ is perfect. Therefore, by Corollary 3.2,

$$m(b_1+3, b_2+3, b_3+3, 3) = m(b_1, b_2, b_3, 3) + m(b_1, 3, 3, 3) + m(3, b_2, 3, 3) + m(3, 3, b_3, 3),$$

and so $(b_1 + 3, b_2 + 3, b_3 + 3)$ is optimal. □

# Chapter 4
# A Tight Bound on Grids of Size $\geq 5$

## 4.1 Introduction and Definitions

Let the ordered tuple $(a, b, c)$ represent the $a \times b \times c$ grid $G$ where $a \geq b \geq c$. We refer to $c$ as the *thickness* of $G$. For example, the tuple $(5, 3, 3)$ represents a $5 \times 3 \times 3$ grid of thickness 3. We refer to a tuple as *divisible*, or a *divisibility case*, if and only if $ab + bc + ca \equiv 0 \pmod 3$. If a tuple is divisible and percolates at the lower bound, we refer to it as *perfect*. Observe that the divisibility cases are precisely those grids with integral lower bounds.

In the following lemmas, we use the notation $(a, b, c) + (x, y, z) = (a+x, b+y, c+z)$ to represent respective increases of $x$, $y$, and $z$ to the side lengths $a$, $b$, and $c$ of $G$. We shall call a thickness *complete* if it can be shown that all divisibility cases in that thickness are perfect. In this section, we demonstrate that thickness 5, thickness 6 and thickness 7 are all complete. As these belong to the residue classes 2, 0, and 1 modulo 3, respectively, we then use a recursive construction to show that all larger grids are also complete.

## 4.2 Completeness of Thickness 5

We show that all divisibility cases for grids of thickness 5 admit perfect lethal sets. Observe that divisibility cases for thickness 5 consist of grids of the form $(x, y, 5)$ where $x$ and $y$ are in residue classes $\{0, 2, 3, 5\}$ modulo 6 (see Table 4.1). We separate these divisibility cases into the following four categories and show that each category is complete:

1. $(x, 5, 5)$ for $x \in \{2, 5\} \pmod 6$;
2. $(x, 6, 5)$ for $x \in \{0, 3\} \pmod 6$;
3. $(x, y, 5)$ for $x, y \in \{0, 2, 3, 5\} \pmod 6$ and $x \not\equiv y$;

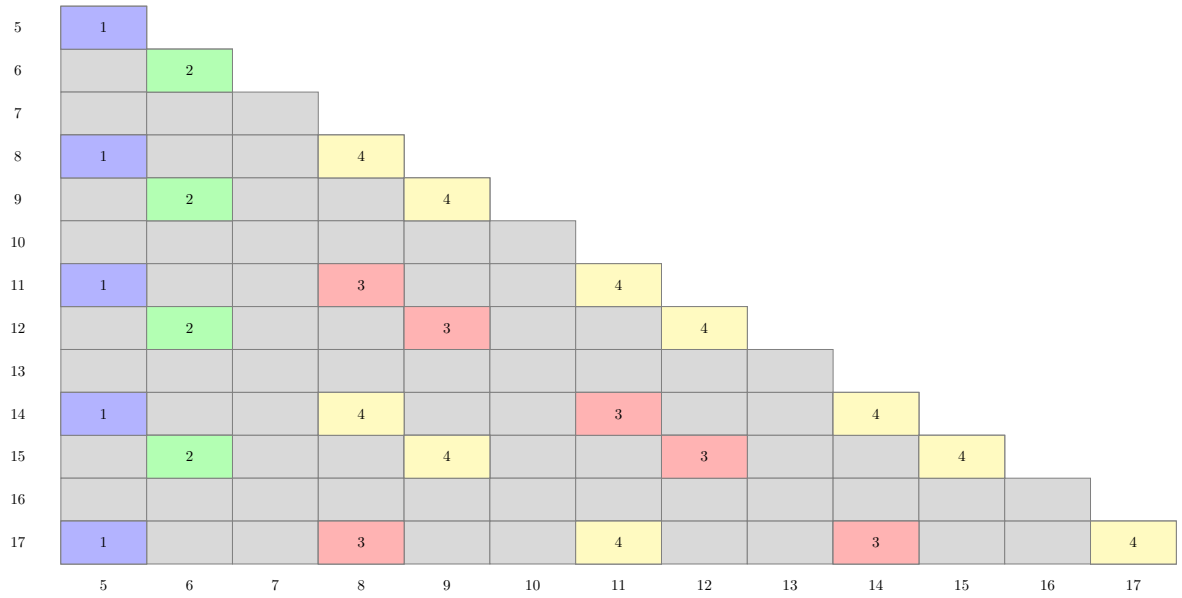


Table 4.1: The four thickness 6 cases analyzed in Lemmas 4.1 (blue), 4.2 (green), 4.3 (red), and 4.4 (yellow).

4. $(x, y, 5)$ for $x, y \in \{0, 2, 3, 5\} \pmod 6$ and $x \equiv y$;

**Lemma 4.1.** *All grids of the form* $(x, 5, 5)$ *for* $x \in \{2, 5\} \pmod 6$ *admit perfect lethal sets.*

*Proof.* Consider the construction $(5, 2, 2) + (a, 3, 3)$, for $a \equiv 0 \pmod 3$ and $a > 3$. Observe that this construction obtains all grids of the form described in (1), apart from $(5, 5, 5)$ and $(8, 5, 5)$.

By Corollary 3.2, we must show that the grids $(5, 2, 2), (5, 3, 3), (a, 2, 3), (a, 3, 2)$ are all perfect. We have that $(5, 2, 2)$ is perfect by Construction A.2 in Appendix A, and $(5, 3, 3)$ is given by Proposition 3.3. Since $a > 3$, Propositions 3.8 and 3.9 give $(a, 2, 3)$.

By Constructions **??** and A.5 in Appendix A, we obtain the remaining grids $(5, 5, 5)$ and $(8, 5, 5)$. We conclude that all grids of the form given in (1) are perfect. □

**Lemma 4.2.** *All grids of the form* $(x, 6, 5)$ *for* $x \in \{0, 3\} \pmod 6$ *admit perfect lethal sets.*

*Proof.* Consider the construction $(6, 3, 2) + (a, 3, 3)$, for $a \equiv 0 \pmod 3$ and $a > 3$. Observe that this construction obtains all grids of the form described in (1), apart from $(6, 6, 5)$ and $(9, 6, 5)$.

By Corollary 3.2, we must show that the grids $(6, 3, 2), (6, 3, 3), (a, 3, 3), (a, 3, 2)$ are all perfect. Since $a > 3$, $(6, 3, 2)$ and $(a, 3, 2)$ are given by Propositions 3.8 and 3.9. Similarly, $(6, 3, 3)$ and $(a, 3, 3)$ are given by Proposition 3.3.

To obtain $(6,6,5)$, we consider the construction $(3,3,1)+(3,3,4)$. By Corollary 3.2, we must show that $(3,3,1),(3,3,4),(3,3,4),(3,3,1)$ are all perfect. These are obtained, respectively, by Propositions 3.3 and 3.7. Construction A.6 gives $(9,6,5)$. We conclude that all grids of the form given in (2) are perfect. □

**Lemma 4.3.** *All grids of the form* $(x,y,5)$ *for* $x,y \in \{0,2,3,5\} \pmod 6$ *and* $x \not\equiv y$ *admit perfect lethal sets.*

*Proof.* Consider the construction $(a,b,2)+(6,6,3)$, for $a,b \in \{0,2,3,5\} \pmod 6$, $a \not\equiv b \pmod 6$, and $a,b > 2$. Observe that this construction obtains all grids of the form described in (3), apart from $(a,8,5)$ for $a \equiv 5 \pmod 6$ and $a \geq 11$.

By Corollary 3.2, we must show that the grids $(a,b,2),(a,6,3),(6,b,3),(6,6,2)$ are all perfect. By Proposition 3.6, $(a,b,2)$ is perfect. Both $(a,6,3)$ and $(6,b,3)$ follow from Proposition 3.4. We obtain $(6,6,2)$ from $(3,3,1)+(3,3,1)$. By Proposition 3.10, $(3,3,1)$ is perfect, and so by Corollary 3.2, $(6,6,2)$ is perfect.

To obtain $(a,8,5)$, for $a \equiv 5 \pmod 6$ and $a \geq 17$, we consider the construction $(8,5,2)+(a,3,3)$, for $a \equiv 3 \pmod 6$ and $a > 3$. By Corollary 3.2, we must show that $(2,5,2)$, $(8,3,3)$, $(a,5,3)$, $(a,2,3)$ are all perfect. We obtain $(2,5,2)$ from Construction A.2 and $(8,3,3)$ from Proposition 3.3. Since $a \equiv 3 \pmod 6$, Proposition 3.6 gives $(a,5,3)$, and Proposition 3.9 gives $(a,2,3)$.

The above construction omits the singular grid $(11,8,5)$. However, we may obtain $(11,8,5)$ from $(2,3,6)+(3,5,5)$. By Corollary 3.2, we must show that $(2,3,6),(2,5,5)$, $(3,3,5),(3,5,6)$ are all perfect. We obtain $(2,5,5)$ from Construction A.3, $(3,3,5)$ from Proposition 3.3, and $(2,3,6)$ and $(3,5,6)$ from Proposition 3.4. We conclude that all grids of the form given in (3) are perfect. □

**Lemma 4.4.** *All grids of the form* $(x,y,5)$ *for* $x,y \in \{0,2,3,5\} \pmod 6$ *and* $x \equiv y$ *admit perfect lethal sets.*

*Proof.* Consider the construction $(a,b,2)+(6,3,3)$, for $a,b \in \{0,2,3,5\} \pmod 6$, $a \not\equiv b \pmod 6$, and $a,b > 2$. Observe that this construction obtains all grids of the form described in (4), apart from $(8,8,5)$.

By Corollary 3.2, we must show that the grids $(a,b,2),(a,3,3),(6,b,3),(6,3,2)$ are all perfect. By Proposition 3.6, $(a,b,2)$ is perfect. Both $(6,3,2)$ and $(6,b,3)$ follow from Proposition 3.4. We obtain $(a,3,3)$ from Proposition 3.3.

To obtain $(8,8,5)$, we consider the construction $(2,2,2)+(6,6,3)$. By Corollary 3.2, we must show that $(2,2,2),(2,6,6),(3,2,6),(3,6,2)$ are all perfect. We obtain $(2,2,2)$ from Construction **??** and $(3,6,2)$ from Proposition 3.4. The construction $(3,3,1)+(3,3,1)$ gives $(6,6,2)$. By Proposition 3.10, $(3,3,1)$ is perfect, and so by Corollary 3.2, $(6,6,2)$ is perfect. We conclude that all grids of the form given in (3) are perfect. □

**Lemma 4.5.** *Thickness 5 is complete.*

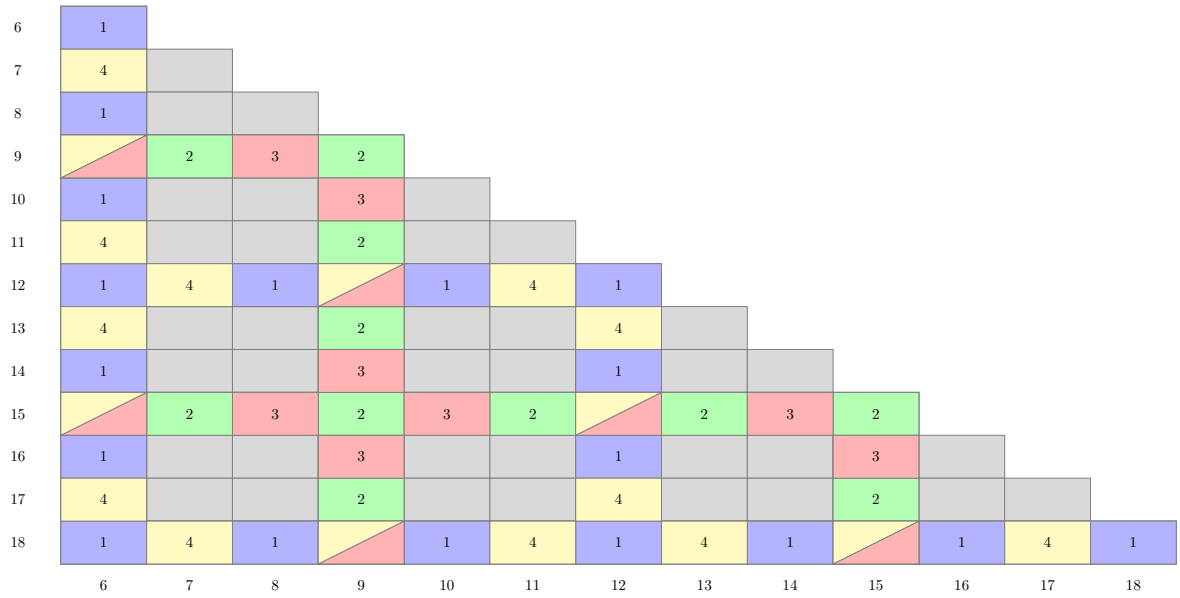


Table 4.2: The four thickness 6 cases analyzed in Lemmas 4.6 (blue), 4.7 (green), 4.8 (red), and 4.9 (yellow).

*Proof.* By Lemmas 4.1, 4.2, 4.3, and 4.4, all divisibility cases for thickness 5 admit perfect lethal sets. □

## 4.3 Completeness of Thickness 6

We show that all divisibility cases for grids of thickness 6 admit perfect lethal sets. Observe that divisibility cases for thickness 6 consist of grids of the form $(x, y, 6)$ where, without loss of generality, $x$ is in residue classes $\{0, 3\}$ modulo 6, and $y$ is either even or odd (see Table 4.2). We separate these divisibility cases into the following four categories and show that each category is complete:

1. $(x, y, 6)$ for $x \equiv 0 \pmod 6$ and $y \equiv 0 \pmod 2$;
2. $(x, y, 6)$ for $x \equiv 3 \pmod 6$ and $y \equiv 1 \pmod 2$;
3. $(x, y, 6)$ for $x \equiv 3 \pmod 6$ and $y \equiv 0 \pmod 2$;
4. $(x, y, 6)$ for $x \equiv 0 \pmod 6$ and $y \equiv 1 \pmod 2$.

**Lemma 4.6.** *All grids of the form $(x, y, 6)$ for $x \equiv 0 \pmod 6$ and $y \equiv 0 \pmod 2$ admit perfect lethal sets.*

*Proof.* Consider the construction $(3n, m, 3)+(3, 3, 3)$, for $n, m \equiv 1 \pmod 2$ and $m > 1$. Observe that this construction obtains all grids of the form described in (1).

By Corollary 3.2, we must show that the grids $(3n, m, 3), (3n, 3, 3), (3, m, 3), (3, 3, 3)$ are all perfect. By Proposition 3.5, $(3n, m, 3)$ is perfect for all $m > 1$. Since $n, m \neq 2$, $(3n, 3, 3), (3, m, 3), (3, 3, 3)$ are all perfect by Proposition 3.3. We conclude that all grids of the form given in (1) are perfect. □

**Lemma 4.7.** *All grids of the form* $(x, y, 6)$ *for* $x \equiv 3 \pmod 6$ *and* $y \equiv 1 \pmod 2$ *admit perfect lethal sets.*

*Proof.* Consider the construction $(3n, m, 3)+(6, 6, 3)$, for $n, m \equiv 1 \pmod 2$ and $m > 1$. Observe that this construction obtains all grids of the form described in (2), apart from $(x, 7, 6)$, for $x \equiv 3 \pmod 6$ and $x \geq 9$.

By Corollary 3.2, we must show that the grids $(3n, m, 3), (3n, 6, 3), (6, m, 3), (6, 6, 3)$ are all perfect. By Proposition 3.5, $(3n, m, 3)$ is perfect for all $m > 1$. Since $n, m > 1$, $(3n, 6, 3), (6, m, 3), (6, 6, 3)$ are all perfect by Proposition 3.4.

To obtain $(x, 7, 6)$, for $x \equiv 3 \pmod 6$ and $x \geq 9$, we consider $(6, 3, 3) + (x-6, 4, 3)$. By Corollary 3.2, we must show that $(6, 3, 3), (6, 4, 3), (x-6, 3, 3), (x-6, 4, 3)$ are all perfect. We obtain $(6, 3, 3)$ and $(x-6, 3, 3)$ from Proposition 3.4. Proposition 3.4 gives $(6, 4, 3)$. Proposition 3.7 gives $(x-6, 4, 3)$. We conclude that all grids of the form given in (2) are perfect. □

**Lemma 4.8.** *All grids of the form* $(x, y, 6)$ *for* $x \equiv 3 \pmod 6$ *and* $y \equiv 0 \pmod 2$*, or* $b \equiv 3 \pmod 6$ *admit perfect lethal sets.*

*Proof.* Consider the construction $(3n, m, 3)+(6, 3, 3)$, for $n, m \equiv 1 \pmod 2$ and $m > 1$. Observe that this construction obtains all grids of the form described in (3).

By Corollary 3.2, we must show that $(3n, m, 3), (3n, 3, 3), (6, m, 3), (6, 3, 3)$ are all perfect. By Proposition 3.5, $(3n, m, 3)$ is perfect for all $m > 1$. Since $m \neq 2$, $(6, m, 3), (6, 3, 3)$ are both perfect by Proposition 3.3. We obtain $(3n, 3, 3)$ by Proposition 3.3. We conclude that all grids of the form given in (3) are perfect. □

**Lemma 4.9.** *All grids of the form* $(x, y, 6)$*, where* $x \equiv 0 \pmod 6$ *and* $y \equiv 1 \pmod 2$ *admit perfect lethal sets.*

*Proof.* Consider the construction $(3n, m, 3)+(3, 6, 3)$, for $n, m \equiv 1 \pmod 2$ and $m > 1$. Observe that this construction obtains all grids of the form described in (4), apart from $(x, 7, 6)$, for $x \equiv 0 \pmod 6$ and $x \geq 6$.

By Corollary 3.2, we must show that the grids $(3n, m, 3)$, $(3n, 6, 3)$, $(3, m, 3), (3, 6, 3)$ are all perfect. By Proposition 3.5, $(3n, m, 3)$ is perfect for all $m > 1$. Since $n, m > 1$, $(3n, 6, 3)$ and $(3, 6, 3)$ are both perfect by Proposition 3.4. Similarly, $(3, m, 3)$ is perfect by Proposition 3.3.

To obtain $(x, 7, 6)$, for $x \equiv 0 \pmod 6$ and $x \geq 6$, we consider $(3, 3, 3) + (x-3, 4, 3)$. By Corollary 3.2, we must show that $(3, 3, 3), (3, 4, 3), (x-3, 3, 3), (x-3, 4, 3)$ are all perfect. We obtain $(3, 3, 3), (3, 4, 3)$ and $(x-3, 3, 3)$ from Proposition 3.3. Since $x \equiv 0$

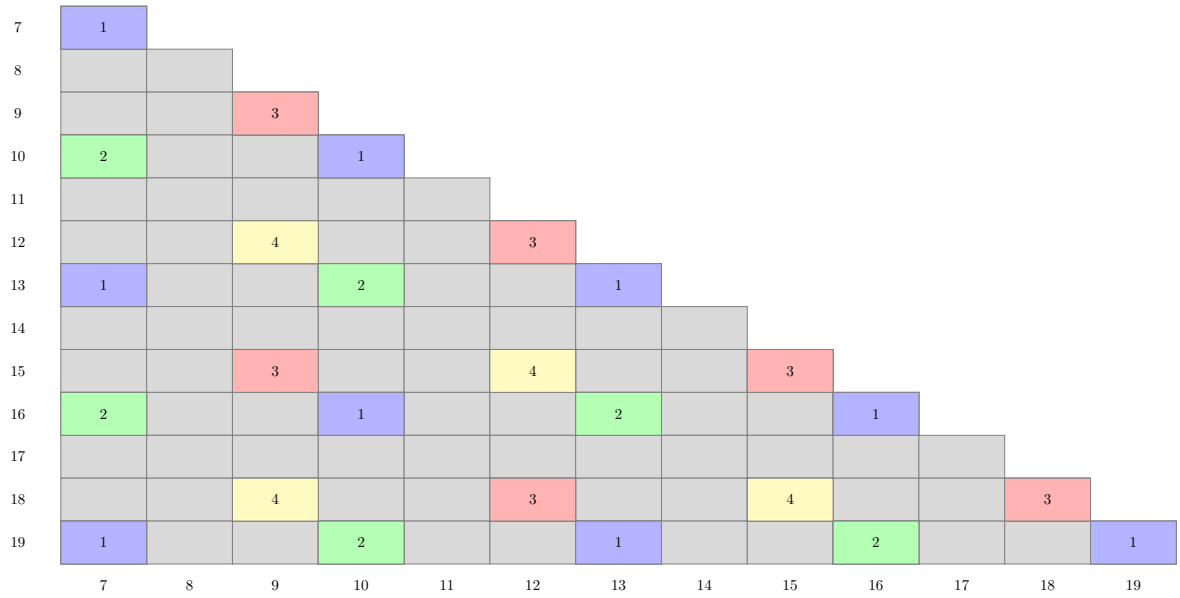


Table 4.3: The four thickness 7 cases analyzed in Lemmas 4.11 (blue), 4.12 (green), 4.13 (red), and 4.14 (yellow).

(mod 6), Proposition 3.7 gives $(x-6, 4, 3)$. We conclude that all grids of the form given in (4) are perfect. □

**Lemma 4.10.** *Thickness 6 is complete.*

*Proof.* All divisibility cases for thickness 6 are grids of the form $(x, y, 6)$ such that at least one of $\{x, y\}$ is congruent to 0 modulo 3. Lemmas 4.6, 4.7, 4.8, and 4.9 cover all such cases. The result follows. □

## 4.4 Completeness of Thickness 7

We show that all divisibility cases for grids of thickness 7 admit perfect lethal sets. Observe that divisibility cases for thickness 7 consist of grids of the form $(x, y, 7)$ for $x, y$ in residue classes $\{0, 1, 3, 4\}$ modulo 6 (see Table 4.3). We separate these divisibility cases into the following four categories and show that each category is complete:

1. $(x, y, 7)$ for $x, y \in \{1, 4\}$ and $x \equiv y \pmod 6$;
2. $(x, y, 7)$ for $x, y \in \{1, 4\}$ and $x \not\equiv y \pmod 6$;
3. $(x, y, 7)$ for $x, y \in \{0, 3\}$ and $x \equiv y \pmod 6$;
4. $(x, y, 7)$ for $x, y \in \{0, 3\}$ and $x \not\equiv y \pmod 6$.

**Lemma 4.11.** *All grids of the form* $(x, y, 7)$ *for* $x, y \in \{1, 4\}$ *and* $x \equiv y \pmod 6$ *admit perfect lethal sets.*

*Proof.* Consider the construction $(a, b, 2) + (8, 5, 5)$ for $a, b \in \{2, 5\} \pmod 6$, $a \not\equiv b \pmod 6$, and $a, b > 2$. Observe that this construction obtains all grids of the form described in (1) above, apart from $(10, 10, 7)$ and $(a, 7, 7)$, for $a \equiv 1 \pmod 6$.

By Corollary 3.2, we must show that the grids $(a, b, 2), (a, 5, 5), (8, b, 5), (8, 5, 2)$ are all perfect. By Proposition 3.6, $(a, b, 2)$ and $(8, 5, 2)$ are perfect. By Lemma 4.5, $(a, 5, 5)$ and $(8, b, 5)$ are perfect.

To obtain $(a, 7, 7)$, for $a \equiv 1 \pmod 6$, we consider $(4, 4, 4) + (a - 4, 3, 3)$. By Corollary 3.2, we must show that $(4, 4, 4), (4, 3, 3), (a-4, 4, 3), (a-4, 3, 4)$ are all perfect. We obtain $(4, 4, 4)$ from $(2, 2, 2)+(2, 2, 2)$. By Construction **??** in Appendix A, we have that $(2, 2, 2)$ is perfect. Proposition 3.3 gives $(4, 3, 3)$. Since $a - 4 \equiv 3 \pmod 6$, we obtain $(a - 4, 4, 3)$ from Proposition 3.7.

To obtain $(10, 10, 7)$, consider $(5, 5, 5) + (5, 5, 2)$. By Corollary 3.2, we must show that $(5, 5, 5), (5, 5, 2), (5, 5, 2), (5, 5, 5)$ are all perfect. Lemma 4.5 gives us $(5, 5, 5)$, and Construction A.3 gives us $(5, 5, 2)$. We conclude that all grids of the form given in (1) are perfect. □

**Lemma 4.12.** *All grids of the form* $(x, y, 7)$ *for* $x, y \in \{1, 4\}$ *and* $x \not\equiv y \pmod 6$ *are complete.*

*Proof.* Consider the construction $(a, b, 2) + (5, 5, 5)$ for $a, b \in \{2, 5\} \pmod 6$, $a \not\equiv b \pmod 6$, and $a, b > 2$. Observe that this construction obtains all grids of the form described in (2) above, apart from $(a, 7, 7)$, for $a \equiv 4 \pmod 6$.

By Corollary 3.2, we must show that the grids $(a, b, 2), (a, 5, 5), (5, b, 5), (5, 5, 2)$ are all perfect. By Proposition 3.6, $(a, b, 2)$ is perfect. We obtain $(a, 5, 5)$ and $(5, b, 5)$ from Lemma 4.5, and $(5, 5, 2)$ is given by Construction A.3.

To obtain $(a, 7, 7)$, for $a \equiv 4 \pmod 6$, we consider $(7, 4, 4) + (a - 7, 3, 3)$. Since $a \equiv 4 \pmod 6$ and $a \geq 7$, we have that $a \geq 10$. By Corollary 3.2, we must show that $(7, 4, 4), (7, 3, 3), (a - 7, 4, 3), (a - 7, 3, 4)$ are all perfect. We obtain $(7, 4, 4)$ from $(2, 2, 2)+(5, 2, 2)$. Constructions **??** and A.2 show that $(2, 2, 2), (2, 2, 2), (5, 2, 2), (5, 2, 2)$ are all perfect. Proposition 3.3 gives us $(7, 3, 3)$. Since $a - 7 \equiv 3 \pmod 6$, we obtain $(a - 7, 4, 3)$ from Proposition 3.7. We conclude that all grids of the form given in (2) are perfect. □

**Lemma 4.13.** *All grids of the form* $(x, y, 7)$ *for* $x, y \in \{0, 3\}$ *and* $x \equiv y \pmod 6$ *are complete.*

*Proof.* Consider the construction $(a, b, 2) + (6, 9, 5)$ for $a, b \in \{0, 3\} \pmod 6$, $a \not\equiv b \pmod 6$, and $a, b > 2$. Observe that this construction contains all grids described in (3) above, apart from $(9, 9, 7)$.

By Corollary 3.2, we must show that the grids $(a, b, 2), (a, 9, 5), (6, b, 5), (6, 9, 2)$ are all perfect. By Proposition 3.6, $(a, b, 2)$ and $(6, 9, 2)$ are perfect. By Proposition 3.5, $(a, 9, 5)$ is perfect. We obtain $(6, b, 5)$ from Lemma 4.5, for $b \geq 5$, and $(6, 3, 5)$ from Proposition 3.4.

To obtain $(9, 9, 7)$, consider $(6, 6, 4) + (3, 3, 3)$. By Corollary 3.2, we must show that $(6, 6, 4), (6, 3, 3), (3, 6, 3), (3, 3, 4)$ are all perfect. We obtain $(6, 6, 4)$ from $(3, 3, 1) + (3, 3, 3)$. Construction A.1 shows that $(3, 3, 1)$ is perfect. Proposition 3.3 gives us $(6, 3, 3)$, $(3, 3, 3)$ and $(4, 3, 3)$. We conclude that all grids of the form given in (3) are perfect. □

**Lemma 4.14.** *All grids of the form* $(x, y, 7)$ *for* $x, y \in \{0, 3\}$ *and* $x \not\equiv y \pmod 6$ *are complete.*

*Proof.* Consider the construction $(a, b, 2) + (6, 6, 5)$ for $a, b \in \{0, 3\} \pmod 6$, $a \not\equiv b \pmod 6$, and $a, b > 2$. Observe that this construction contains all grids described in (4) above.

By Corollary 3.2, we must show that the grids $(a, b, 2), (a, 6, 5), (6, b, 5), (6, 6, 2)$ are all perfect. By Proposition 3.6, $(a, b, 2)$ is perfect. We obtain $(6, b, 5)$ from Lemma 4.5, for $b \geq 5$, and $(6, 3, 5)$ from Proposition 3.4. We obtain $(6, 6, 2)$ from $(3, 3, 1) + (3, 3, 1)$. By Proposition 3.10, $(3, 3, 1)$ is perfect, and so by Corollary 3.2, $(6, 6, 2)$ is perfect. We conclude that all grids of the form given in (4) are perfect. □

**Lemma 4.15.** *Thickness 7 is complete.*

*Proof.* By Lemmas 4.11, 4.12, 4.13, and 4.14, all divisibility cases for thickness 7 admit perfect lethal sets. □

## 4.5 Proof of the Main Result

We are now in a position to prove Theorem 1.6. We first state the following auxiliary result for divisibility cases.

**Corollary 4.16.** *Let* $(a_1, a_2, a_3)$ *be a divisibility case, for* $a_1 \geq a_2 \geq a_3 \geq 5$. *Then* $(a_1, a_2, a_3)$ *admits a perfect lethal set.*

*Proof.* By Lemmas 4.5, 4.10, and 4.4, all divisibility cases for $(a_1, a_2, 5)$, $(a_1, a_2, 6)$, and $(a_1, a_2, 7)$ admit perfect lethal sets. Observe that $(a_1, a_2, a_3) + (3, 3, 3)$ gives a one-to-one mapping from divisible grids of thickness $a_3$ to divisible grids of thickness $a_3 + 3$. By Lemma 3.11, if $(a_1, a_2, a_3)$ admits a lethal set, then $(a_1, a_2, a_3) + (3, 3, 3)$ admits a lethal set. Therefore, since each residue class modulo 3 is complete, all divisibility cases $(a_1, a_2, a_3)$, for $a_1 \geq a_2 \geq a_3 \geq 5$, admit perfect lethal sets. □

| mod 3 | ≡ 2 | ≡ 0 | ≡ 1 |
|---|---|---|---|
| ≡ 2 | | $(5,6,5)$<br>$(2,0,2)$ | $(5,7,5)$<br>$(2,1,2)$ |
| ≡ 0 | $(6,5,5)$<br>$(0,2,2)$ | | $(6,7,5)$<br>$(0,1,2)$ |
| ≡ 1 | $(7,5,5)$<br>$(1,2,2)$ | $(7,6,5)$<br>$(1,0,2)$ | $(7,7,5)$<br>$(1,1,2)$ |

| mod 3 | ≡ 0 | ≡ 1 | ≡ 2 |
|---|---|---|---|
| ≡ 0 | | | |
| ≡ 1 | | $(7,7,6)$<br>$(1,1,0)$ | $(7,8,6)$<br>$(1,2,0)$ |
| ≡ 2 | | $(8,7,6)$<br>$(2,1,0)$ | $(8,8,6)$<br>$(2,2,0)$ |

| mod 3 | ≡ 1 | ≡ 2 | ≡ 0 |
|---|---|---|---|
| ≡ 1 | | $(7,8,7)$<br>$(1,2,1)$ | $(7,9,7)$<br>$(1,0,1)$ |
| ≡ 2 | $(8,7,7)$<br>$(2,1,1)$ | $(8,8,7)$<br>$(2,2,1)$ | $(8,9,7)$<br>$(2,0,1)$ |
| ≡ 0 | $(9,7,7)$<br>$(0,1,1)$ | $(9,8,7)$<br>$(0,2,1)$ | |

Table 4.4: Residue tuples for non-divisibility cases in thicknesses 5, 6, and 7. Top tuple is grid dimension, bottom tuple is residues modulo 3.

The proof of Theorem 1.6 requires further implementation of the recursive process outlined in Lemma 3.1. In particular, we leverage Corollary 4.16 to prove the following helpful lemma:

**Lemma 4.17.** *Let $(a_1, a_2, a_3)$ be any grid such that $a_1 \geq a_2 \geq a_3 \geq 5$. If $(a_1, a_2, a_3)$ is optimal, then $(a_1, a_2, a_3) + (3b_1, 3b_2, 3b_3)$ is optimal for $b_1, b_2, b_3 \geq 2$.*

*Proof.* By Corollary 3.2, we must show that $(a_1, 3b_2, 3b_3), (3b_1, a_2, 3b_3), (3b_1, 3b_2, a_3)$ are all perfect. Since $3b_1 \equiv 3b_2 \equiv 3b_3 \equiv 0 \pmod 3$, each of these grids is divisible. Furthermore, each grid has minimum thickness 5 and so, by Corollary 4.16, each grid is perfect. □

Let $(r_1, r_2, r_3)$ be the tuple of residues of $(a_1, a_2, a_3)$ modulo 3. Given an optimal grid $(a_1, a_2, a_3)$, Lemma 4.17 says that all other grids of size at least $(a_1{+}6, a_2{+}6, a_3{+}6)$ with the same $(r_1, r_2, r_3)$ are optimal. Therefore, by obtaining optimal lethal sets on the smallest grids for each residue tuple $(r_1, r_2, r_3)$, we are able to obtain a lower bound on the size of all optimal grids under 3-neighbor percolation (see Table 4.4).

*Proof of Theorem 1.6.* Let $(a_1, a_2, a_3)$ be such that $a_1 \geq a_2 \geq a_3 \geq 11$. Observe that each $a_i$ can be written as $3b_i + r_i$, for $b_i \geq 2$ and some $r_i \in \{5, 6, 7\}$. We therefore have that $(a_1, a_2, a_3) = (r_1, r_2, r_3) + (3b_1, 3b_2, 3b_3)$, for $r_1, r_2, r_3 \in \{5, 6, 7\}$. By Lemma 4.17, $(a_1, a_2, a_3)$ is optimal if $(r_1, r_2, r_3)$ is optimal.

Corollary 4.16 gives us the optimality of divisibility cases. Therefore, we need only consider non-divisible grids $(r_1, r_2, r_3)$. In particular, we must show that $(6, 5, 5)$, $(7, 5, 5)$, $(7, 6, 5)$, $(7, 7, 5)$ and $(7, 7, 6)$ are all optimal. We obtain $(7, 7, 6)$ from $(4, 4, 3)+$ $(3, 3, 3)$. By Lemma 3.11, $(7, 7, 6)$ is optimal. Constructions for $(6, 5, 5)$, $(7, 5, 5)$, $(7, 6, 5)$, $(7, 7, 5)$ are given in Appendix A.

Since each of the non-divisibility grids $(r_1, r_2, r_3)$ admits an optimal lethal set, we conclude that all grids $(a_1, a_2, a_3)$ where $a_1 \geq a_2 \geq a_3 \geq 11$ are optimal. □

# Chapter 5
# Thickness One

While results from the previous chapters resolve the question of $m(a_1, a_2, a_3, 3)$ for $a_1 \geq a_2 \geq a_3 \geq 11$, similar constructions for smaller grids remain sparse. Nevertheless, computer examples seem to suggest that grids of minimum size at least 2 are largely optimal. Grids of thickness 1 tell a different story. In this chapter, we prove that the only perfect grids in thickness 1 are those of the form $[2^n - 1]^2$. This answers a question posed by Benevides et al. in [**?**].

## 5.1 A tight result for $[n]^2$

The argumentative structure of the proof is as follows: Let $A_0$ be a perfect lethal set on the grid $(a_1, a_2, 1)$. We show that the structure of $A_0$ guarantees the existence of a perfect lethal set on the smaller grid $(\frac{a_1-1}{2}, \frac{a_2-1}{2}, 1)$. Repeated applications of this process of reduction guarantee the existence of a perfect lethal set on the grid $(a_0, 1, 1)$. Since the only such grid that admits a perfect lethal set is $(1, 1, 1)$, we are forced to conclude that $a_1 = a_2 = 2^k - 1$ for some $k > 0$.

### 5.1.1 Preliminaries

For the remainder of the chapter, let $G = [a_1] \times [a_2]$. Recall that perfect lethal sets match the surface area bound. In particular,

$$|A_0| = \frac{a_1 a_2 + a_1 + a_2}{3}.$$

We begin with the following observations regarding the structure of $A_0$:

**Proposition 5.1.** *If $A_0$ is a perfect lethal set on $G$, then $A_0$ contains alternating vertices along the border of $G$.*

*Proof.* Since $A_0$ is perfect, it must form an independent set in $G$. By Proposition 2.6, no two adjacent border vertices are both uninfected. Together, these conditions ensure that $A_0$ intersects the border of $G$ in an alternating pattern (see Figure 5.2). □

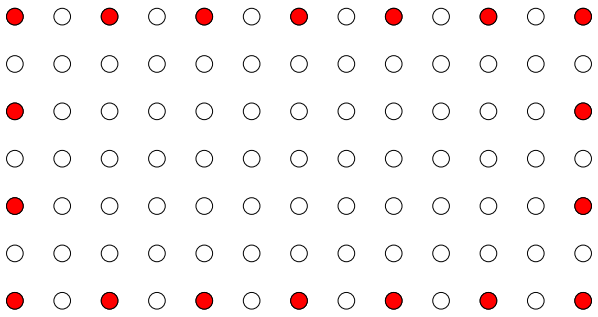

Figure 5.1: Alternating infection along the border of $[7] \times [13]$.

**Proposition 5.2.** *If $A_0$ is a perfect lethal set on $G$, then $a_1, a_2 \equiv 1 \pmod 2$.*

*Proof.* By Propositions 5.1 and 2.5, $a_1, a_2 \equiv 1 \pmod 2$. □

**Proposition 5.3.** *Let $A_0$ be a perfect lethal set on $[a_1] \times [a_2]$ under 3-neighbor percolation. Let $H = V([a_1] \times [a_2]) \setminus A_0$. Then the subgraph induced by $H$ is acyclic and each component of $H$ contains exactly one border vertex.*

*Proof.* Sufficiency follows from Proposition 2.7. For necessity, observe that the interior vertices of $A_0$ each remove exactly 4 edges from the subgraph induced by $H$. This implies that the subgraph induced by $H$ is a forest with exactly $a_1 + a_2 - 2$ components. As there are exactly $a_1 + a_2 - 2$ border vertices in $H$, each component must contain exactly one border vertex. □

Consider a labeling of the vertices of $G$ by their coordinates, starting at $(1, 1)$ in the lower left and ranging to $(a_1, a_2)$ in the upper right. Refer to a vertex $(x, y)$ as "even" or "odd" depending on the parity of $x + y$. If a set $S \subseteq V(G)$ contains all vertices of the same parity, call $S$ monochromatic. The following lemma leverages the prior propositions to prove that any perfect lethal set on $G$ must be monochromatic.

**Lemma 5.4.** *Let $A_0$ be a perfect lethal set on $G$. Then $A_0$ is monochromatic with respect to the proper 2-coloring of $G$.*

*Proof.* From Proposition 5.1, observe that $A_0$ contains all even vertices along the border of $G$. Suppose for contradiction that $A_0$ also contains odd vertices. We show that this implies the existence of a cycle in the subgraph induced by $V(G) \setminus A_0$, contradicting Proposition 5.3.

Let $H$ be a graph with vertices $V(H) = V(G)$ and edges $uv$ if and only if $u$ and $v$ are diagonally adjacent in $G$. Consider the subgraph of $H$ induced by the odd vertices of $A_0$ and let $K$ be a connected component. Observe that $K$ is acyclic: any cycle in $K$ encloses a component of $G[\overline{A_0}]$, contradicting Proposition 5.3. Furthermore, by Proposition 5.1, all vertices of $K$ are in the interior of $G$. Let $C_H$ be the cycle induced in $H$ by $N_G(K)$. Note that since $A_0$ is an independent set, $N_G(K) \cap A_0 = \emptyset$ and $C_H \cap A_0 = \emptyset$. Consider

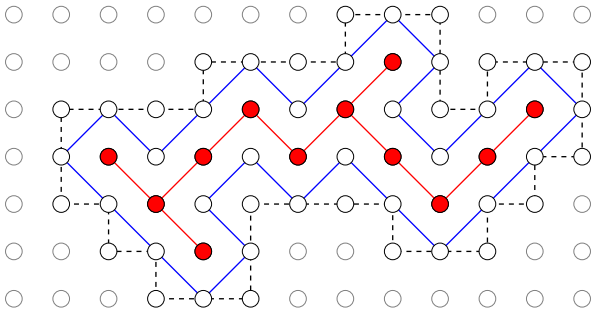

Figure 5.2: $[7] \times [13]$ grid with component $K$ (red), $C_H$ (blue), and $C_G$ (dashed).

the closed walk induced in $G$ by the vertices $V(C_H) \cup N_H(K) \setminus A_0$. This walk describes a cycle $C_G$ in $G[\overline{A_0}]$, which contradicts Proposition 5.3. □

### 5.1.2 Reduction

We present an auxiliary $(\frac{a_1-1}{2}, \frac{a_2-1}{2}, 1)$ grid $G'$ obtained from $G$, and show that it admits a perfect lethal set. Let the vertices of $G'$ be $2 \times 2$ tiles of $G$ given by

$$\{(2x-1, 2y-1), (2x-1, 2y), (2x, 2y-1), (2x, 2y) \mid (x, y) \in [1, (a_1-1)/2] \times [1, (a_2-1)/2]\},$$

with adjacencies between tiles that differ by one in each of the cardinal directions. Note that Proposition 5.2 ensures that $|V(G')|$ is an integer. Furthermore, observe that for any tile $T_{x,y} \in V(G')$, $|A_0 \cap T_{x,y}| \in \{1, 2\}$. This follows from the fact that $A_0$ is an independent set, and $G[\overline{A_0}]$ is acyclic. For all $T_{x,y} \in V(G')$, color $T_{x,y}$ blue if $|A_0 \cap T_{x,y}| = 2$, and white otherwise. Let $b$ and $w$ be the number of blue and white tiles in $V(G')$, respectively. We determine $b$ by solving the following system of equations:

$$\begin{aligned} b + w &= \frac{(a_1 - 1)(a_2 - 1)}{4} \\ 2b + w &= \frac{a_1 a_2 + a_1 + a_2}{3} - \frac{a_1 + a_2}{2}. \end{aligned}$$

This gives the following expression for $b$:

$$\frac{a_1 a_2 + a_1 + a_2}{3} - \frac{a_1 + a_2}{2} - \frac{(a_1 - 1)(a_2 - 1)}{4} = \frac{a_1 a_2 + a_1 + a_2 - 3}{12} \tag{5.1}$$

$$= \frac{(\frac{a_1-1}{2})(\frac{a_2-1}{2}) + \frac{a_1-1}{2} + \frac{a_2-1}{2}}{3}. \tag{5.2}$$

Note that this is precisely the surface area bound for the $(\frac{a_1-1}{2}, \frac{a_2-1}{2}, 1)$ grid. Furthermore, since $a_1 \equiv a_2 \equiv 1 \pmod 6$ or $a_1 \equiv a_2 \equiv 3 \pmod 6$, all terms on the LHS of 5.1 are integral, and so the SA bound in 5.2 is tight.

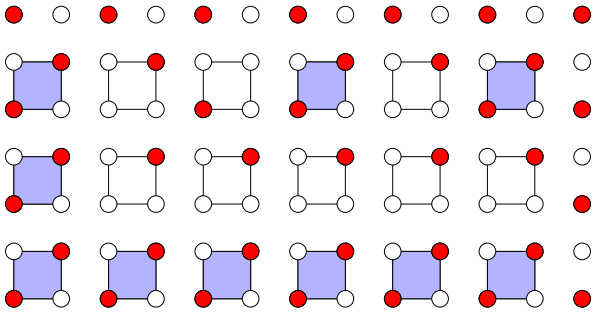

Figure 5.3: $[7] \times [13]$ grid with $T_{x,y}$ colored blue if $|T_{x,y} \cap A_0| = 2$. Note that $A_0$ is *not* perfect.

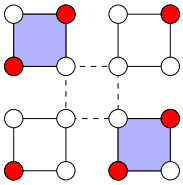

Figure 5.4: Diagonal white tiles and the resulting 4-cycle.

We prove that the blue tiles form a lethal set in $G'$. We begin with the following observation:

**Proposition 5.5.** *All white tiles have their $A_0$-vertex in the bottom left corner.*

*Proof.* For contradiction, suppose that there exists a white tile $T_0$ with one infected vertex in the upper right. By Proposition 5.3, there exists a path in $G[\overline{A_0}]$ from $T_0 \setminus A_0$ to the border. We consider the sequence of white tiles $T_0, \ldots, T_n$ containing this path.

Consider two consecutive tiles $T_i, T_{i+1}$ in this sequence. Note that $T_i$ and $T_{i+1}$ cannot be diagonally adjacent, as such a configuration creates a 4-cycle in $G[\overline{A_0}]$ (see Figure 5.4). Additionally, by Proposition 5.1, observe that $T_n$ has its infected vertex in the bottom left corner. Therefore, since $T_0$ contains an infection in the top right by assumption, there exist tiles $T_i, T_{i+1}$ such that $T_i$ has an infection in the top right, and $T_{i+1}$ has an infection in the bottom left.

We consider two cases. If $T_{i+1}$ is below or to the left of $T_i$, we obtain a 4-cycle. On the other hand, if $T_{i+1}$ is above or to the right of $T_i$, there is no path in $G[\overline{A_0}]$ between them (see Figure 5.5). We therefore conclude that $T_0$ must have an infected vertex in the bottom left. □

We are now prepared to prove that the blue tiles form a lethal set in $G'$.

**Lemma 5.6.** *The set of blue tiles is lethal and perfect in $[(a_1 - 1)/2] \times [(a_2 - 1)/2]$ under 3-neighbor percolation.*

*Proof.* In Equation 5.2, we saw that the number of blue tiles matches the lower bound for 3-neighbor percolation in $[(a_1 - 1)/2] \times [(a_2 - 1)/2]$. We now show that the 3-

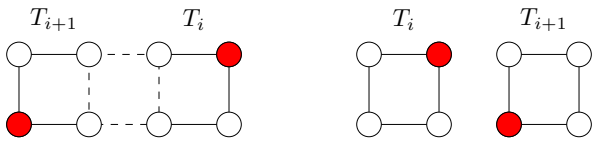


Figure 5.5: Possible configurations of adjacent white tiles.

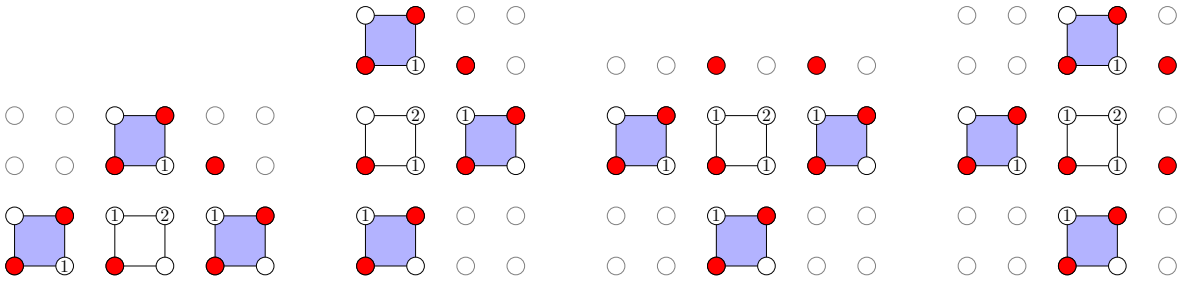

Figure 5.6: The four configurations of blue tiles leading to infection.

neighbor process infects white tiles if and only if they are adjacent to at least 3 blue tiles.

For sufficiency, consider the four cases illustrated in Figure 5.6. In each of these configurations, the upper right vertex of the white tile (labeled with a "2") becomes infected after two iterations. Each case requires the assistance of one to two extra infections outside of the three blue tiles. However, these infections constitute the bottom left vertex in adjoining tiles, which is always infected.

For necessity, we show that any cycle or border-to-border path in the white tiles of $G'$ implies a cycle or border-to-border path in $G[\overline{A_0}]$. Observe that, by Proposition 5.5, the vertices $(T_i \cup T_j) \setminus A_0$ of any adjacent white tiles $T_i, T_j$ induce a connected component in $G$. Therefore, any cycle or border-to-border path in $G'$ implies the existence of a cycle or border-to-border path in $G[\overline{A_0}]$. We conclude that the blue tiles form a perfect lethal set in $[(a_1-1)/2] \times [(a_2-1)/2]$ under 3-neighbor percolation. $\square$

We have shown that the existence of a perfect lethal set on $[a_1] \times [a_2]$ implies the existence of a perfect lethal set on $[(a_1-1)/2] \times [(a_2-1)/2)]$. Proposition 5.2 mandates that all perfect lethal sets on $[a_1] \times [a_2]$ be odd-by-odd. Together, these statements require that $a_1 = 2^{k_1} - 1$ and $a_2 = 2^{k_2} - 1$ for some $k_1, k_2 > 0$, respectively. By repeated applications of Lemma 5.6, we ultimately obtain a grid $[a_0] \times [1]$ that admits a perfect lethal set. Clearly, the only such grid is the single vertex [1]. We therefore conclude that the only two-dimensional grids that admit perfect lethal sets under 3-neighbor percolation are square grids of the form $[2^n - 1]^2$. A construction that achieves this is published in Benevides et al [**?**], and reproduced below.

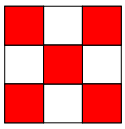

Figure 5.7: A perfect percolating set for $(3, 3, 1)$.

### 5.1.3 Purina

We refer to this construction colloquially as the Purina construction, due to the similarly between its instance on the $(3, 3, 1)$ grid and the logo of the pet food brand. No funding has been offered, but we are open to the possibility. A more extensive discussion on this pattern can be found in [2].

**Construction 5.7.** *All grids of the form* $(2^n - 1, 2^n - 1, 1)$ *are perfect.*

*Proof.* This is a recursive construction built from the base component piece shown in Figure 5.7. Note that this $(3, 3, 1)$ construction is lethal under the 3-neighbor bootstrap process, and that it meets the surface area bound:

$$\frac{1}{3} \cdot (ab + bc + ca) = \frac{1}{3} \cdot (9 + 3 + 3) = 5.$$

For larger grids of size $(2^n - 1, 2^n - 1, 1)$, join four copies of $(2^{n-1} - 1, 2^{n-1}, 1)$ about two perpendicular corridors, and infect the vertex at their intersection (Figure 5.8). Observe that the resulting set is lethal: each of the four smaller grids is lethal by hypothesis, and the remaining vertices induce a forest with disconnected boundary points, which percolates by Proposition 2.7. Furthermore, note that

$$\begin{aligned} \text{S.A.}(2^n - 1, 2^n - 1, 1) &= \frac{1}{3} \cdot (2^{2n} - 1) \\ &= 4 \cdot \frac{1}{3} \cdot (2^{2n-2} - 1) + 1 = 4 \cdot \text{S.A.}(2^{n-1} - 1, 2^{n-1}, 1) + 1, \end{aligned}$$

and therefore this construction is perfect. □

Although the only two-dimensional grids that admit perfect lethal sets under 3-neighbor percolation are square grids of the form $[2^n - 1]^2$, there is at least one family of two-dimensional grids that admits optimal lethal sets. We examine these grids in the following chapter, and note that their existence is of particular value in our analysis of other infinite families of grids that admit perfect lethal sets.

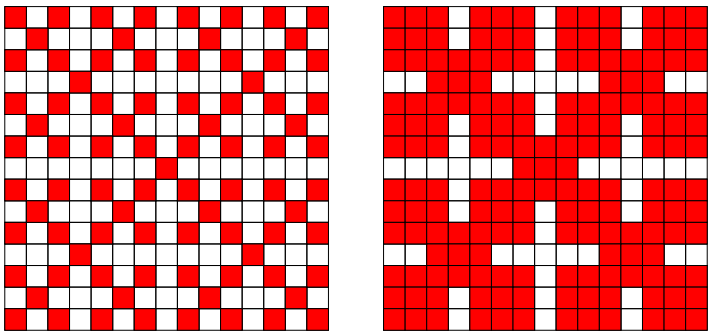

Figure 5.8: A perfect percolating set for $(15, 15, 1)$.

# Chapter 6
# Constructions

## 6.1 Introduction

In this chapter, we present diagrammed proofs of grids that admit optimal and perfect lethal sets under the 3-neighbor process. The proofs are organized by the thickness of the grid. All constructions in the following sections belong to infinite families of grids. We use two strategies in our analysis of these constructions, dependent on the parity of the grid.

We examine families of the form $(0, 1, 1) \pmod 2$ by region, and observe that certain regions can be expanded to arbitrarily large sizes without adversely affecting the spread of infection. In particular, we split these grids into components $A, B, X$, where $A$ and $B$ bookend a central, repeating segment $X$. Our discussion will make use of the following definition and lemma:

**Definition 6.1.** For a grid $G = [a_1] \times [a_2] \times [a_3]$, define the $k$th *level* of $G$ as the subgraph $L_k = [a_1] \times [a_2] \times \{k\}$, for $k \in [a_3]$.

**Lemma 6.2.** *Let $G = [a_1] \times [a_2] \times [a_3]$ and let $L_k$ be the $k$th level of $G$. Suppose all vertices in $L_k$ are infected. Then any lethal set in $L_{k+1}$ (resp. $L_{k-1}$) under the 2-neighbor process is lethal in $G[V(L_k) \cup V(L_{k+1})]$ (resp. $G[V(L_{k-1}) \cup V(L_k)]$) under the 3-neighbor process.*

*Proof.* Each vertex $v \in L_{k+1} \cup L_{k-1}$ has an infected neighbor in $L_k$. Therefore, if $v$ has two infected neighbors in its own level, it has at least 3 infected neighbors in $G$. □

Proofs of the lethality of the remaining families all leverage Lemma 2.1. As a consequence, their argumentative structure remains broadly the same, even as the constructions themselves appear quite different. We shall outline this structure here, before examining the specific proofs.

We begin by demonstrating that the grid $G = (a_1, a_2, a_3)$ admits a manifold $M$. Recall from Corollary 2.2 that a manifold on $G$ is the union of faces

$$F_{1,k_1} \cup F_{2,k_2} \cup F_{3,k_3}$$

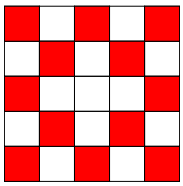

Figure 6.1: An optimal percolating set for $(5, 5, 1)$.

for some $k_i \in [a_i]$. To show that a particular subset $M$ of $V(G)$ is a manifold, we identify the regions $R_1, \ldots, R_n$ that partition $V(G) \setminus M$ and are flanked by three perpendicular walls. In our diagrams, these regions are represented by the volumes bordered by three perpendicular blue, green, and red walls. We then identify a proper unfolding $H$ of $M$ and show that $H$ admits a lethal set $A$, where $|A| = \mathrm{SA}(G)$. Finally, we apply Corollary 2.2 to prove that $G$ is perfect.

## 6.2 Thickness 1

We present a construction that is optimal on all grids $(a, b, 1)$, where $a \equiv 5 \pmod 6$, $b \equiv 1 \pmod 2$, and $a, b \geq 5$. As such grids constitute non-divisibility cases, this construction is not perfect. However, by leveraging Lemma 2.4, we shall see that it can be used to obtain perfect lethal sets on certain grids of thickness 3.

As indicated by Proposition 2.7, a fundamental characteristic of lethal sets $A_0$ is the presence of an initially uninfected corridor, bounded by walls of infection. This structure is apparent in the second diagrams of Figures 5.8 and 6.3 in the previous chapter. These corridors correspond to forests in the complement $G[\overline{A_0}]$ of $A_0$. In this section, we provide a general method for constructing such corridors in $(a, b, 1)$ grids where $a \equiv 5 \pmod 6$ and $b \equiv 1 \pmod 2$.

**Construction 6.3.** *All grids of the form* $(a, b, 1)$*,* $a \equiv 5 \pmod 6$*,* $b \equiv 1 \pmod 2$*, and* $a, b \geq 5$ *are optimal.*

*Proof.* For grids of the form $(a, b, 1)$, $a \equiv 5 \pmod 6$, $b \equiv 1 \pmod 2$, we construct an optimal infected set and show that it is lethal by Proposition 2.7. For the base case, consider the $(5, 5, 1)$ grid $G$ illustrated in Figure 6.1. Observe that this construction is optimal. Now consider the grid $G'$ resulting from the insertion of a $(5, 2k, 1)$ block, as shown in Figure 6.2. Note that the subgraph induced by the uninfected vertices of $G'$ satisfies the conditions of Proposition 2.7. Furthermore, note that if any $(5, n, 1)$ grid is optimal, the $(5, n + 2, 1)$ grid resulting from such a construction has surface area bound $\mathrm{S.A.}(5, n, 1) + 4$, which agrees with the number of infected vertices.

To extend this construction in the vertical direction, we introduce a kink in the snaking infection. This kink requires six rows to produce a repeating pattern. The structure of this design is shown in Figure 6.3. For grids of smaller width, the same

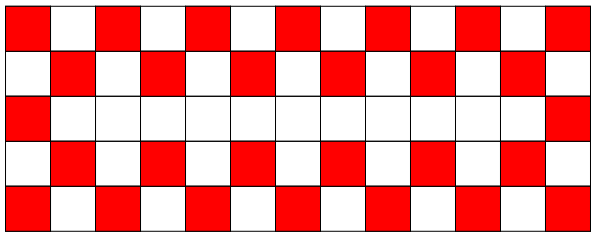

Figure 6.2: An optimal percolating set for $(5, 13, 1)$.

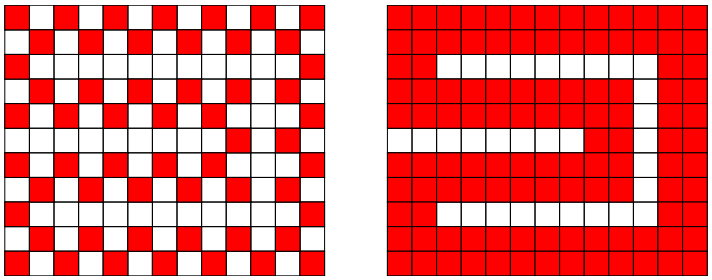

Figure 6.3: An optimal percolating set for $(11, 13, 1)$.

construction gives optimal percolating sets; however, the snaking pattern is increasingly difficult to recognize in thin grids. □

## 6.3 Thickness 2

We examine four infinite families of perfect grids and show that each has a manifold that admits a lethal set of perfect size. We note that such lethal sets are likely to exist for nearly all divisibility cases in thickness two; however, constructions are elusive and those presented here are sufficient to prove the main result of this thesis.

**Construction 6.4.** *All* $(a, 3, 2)$ *grids with* $a \equiv 3 \pmod 6$ *and* $a > 3$ *are perfect.*

*Proof.* Let $G = (6k + 3, 3, 2)$ be a grid such that $k > 0$. Let $A = \{1\} \times [3] \times [2]$, $B = \{6k+2, 6k+3\} \times [3] \times [2]$, and $X_i = \{6i+2, 6i+3, 6i+4, 6i+5, 6i+6, 6i+7\} \times [3] \times [2]$ for $i \in [k-1] \cup \{0\}$, be components of $G$. Denote by $AX^kB$ the union of components $A \cup X_0 \cup \cdots \cup X_{k-1} \cup B$, and note that $G = AX^kB$. Let $A_t^k \subseteq V(G)$ be the set of infectious vertices in $G$ at time $t$, and suppose that each $X_i$ contains the same pattern of infected vertices (see Figure 6.4). We show that $A_0^k$ is lethal and perfect.

Consider the union of components $AX^k = A \cup X_0 \cup \cdots \cup X_{k-1}$ (see Figure 6.5). Let $L_1$ and $L_2$ be the top and bottom levels $AX^k$, respectively. Observe that after one time-step, the subgraph $L_1[\overline{A_1^k}]$ is a forest connected to the border of $L_1$, and so by Proposition 2.7, $A_0^k$ is lethal on $L_1$.

Now consider $G$ and observe that the top level becomes fully infected (see Figure 6.6). Therefore, by Lemma 6.2, it is sufficient to prove that $A_0^k$ is lethal on the bottom

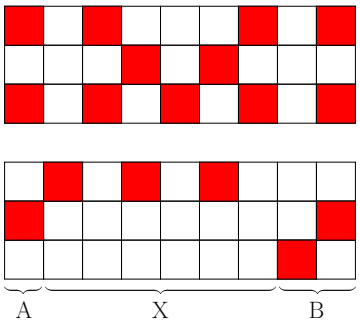


Figure 6.4: The components $A$, $X$, $B$ on $G = AXB$ with infectious set $A_0$.

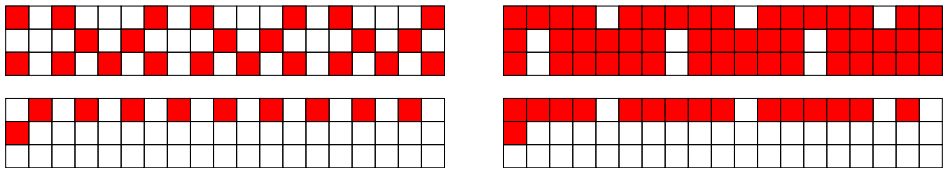

Figure 6.5: An infection on $AX^3$, $t = 0$ and $t = 1$.

level under the 2-neighbor bootstrap process. Figure 6.7 illustrates the key steps of this process on the smaller grid $AXB$, starting at $t = 1$. Infection spreads down rows delineated by red arrows, ultimately infecting all vertices in the bottom level. We conclude that $A_0^k$ is lethal on $G$ under the 3-neighbor process.

To prove that $A_0^k$ is perfect, observe that $|A_0^k| = 3 + 10k + 4$. The surface area bound for $G = (6k + 3, 3, 2)$ is given by

$$\frac{(3)(6k+3) + (3)(2) + (2)(6k+3)}{3} = \frac{30k + 21}{3} = 10k + 7.$$

Since these two values are equal, $A_0^k$ is tight and lethal, and therefore perfect. □

**Construction 6.5.** *All* $(a, 3, 2)$ *grids with* $a \equiv 0 \pmod 6$ *and* $a \geq 6$ *are perfect.*

*Proof.* Let $G$ be an $(a, 3, 2)$ grid with $a \equiv 0 \pmod 6$ and $a \geq 6$, and let $M$ be a manifold of $G$ and $H$ be its proper unfolding (see Figure 6.8). Observe that $M$ is indeed a manifold: it partitions $V(G) \setminus M$ into two sets $R_1$ and $R_2$, both bounded by mutually orthogonal red, green, and blue faces (see Figure 6.8a). Furthermore, note

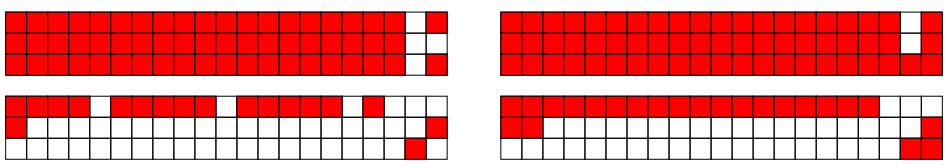

Figure 6.6: An infection on $G$.

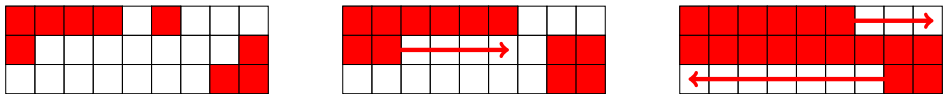

Figure 6.7: The 2-neighbor process on $(9, 3, 1)$ for $t = 1$, $t \in \{2, 3, 4, 5, 6\}$, and $t \in \{7, 8, 9, 10, 11, 12, 13, 14\}$.

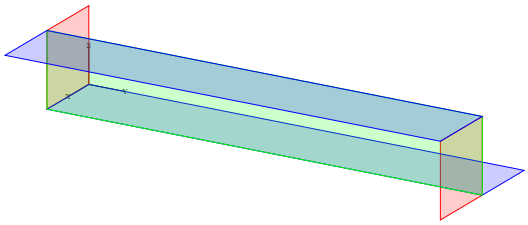

(a) A manifold of $G = (3, 12, 2)$.

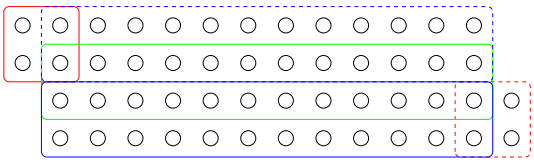

(b) A proper unfolding of $G$.

Figure 6.8: A proper unfolding of $G = (3, 12, 2)$. Colored rectangles indicate faces of $G$. Dashed lines indicate that cells appear on different layers.

that $H$ is obtained from $M$ by cutting along seams between red and green faces, and flattening the figure. It follows that $H$ is a proper unfolding of $G$.

Let $X_1, \ldots, X_k$ be the repeated components of $H$. Denote by $X$ the union of these components. Let $A_t \subseteq V(H)$ be the set of infectious vertices in $H$ at time $t$, and suppose that each $X_i$ contains the same pattern of infected vertices (see Figure 6.9). We show that $A_0$ is lethal and perfect.

Consider an initial infection $A_0$ of $H$ (see Figure 6.9). Observe that $A_0$ infects all vertices of $X$ by Proposition 2.7. We show that the remaining healthy vertices of $H$ become infected. Consider re-folding $H$, and note that the two cells marked with an "X" in $H$ represent the same cell in $G$. This is enough to infect the remaining regions of $H$, and by Corollary 2.2, $A_0$ is lethal on $G$.

To prove that $A_0$ is perfect, observe that $|A_0| = 4+10k+8 = 10k+12$. The surface area bound for $G = (6k + 6, 3, 2)$, where $k$ is the number of repeated components $X$, is given by

$$\frac{(3)(6k+6) + (3)(2) + (2)(6k+6)}{3} = \frac{30k+36}{3} = 10k + 12.$$

Since these two values are equal, $A_0$ is tight and lethal, and therefore perfect. □

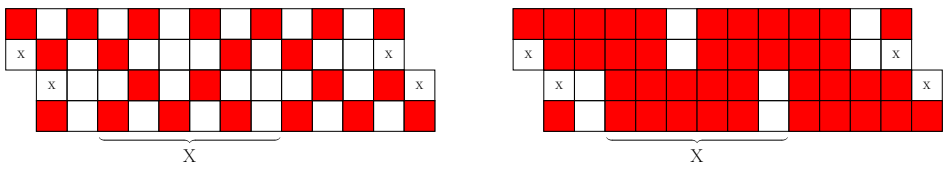


Figure 6.9: A lethal set on $H$ showing the repeated component $X$ ($t = 1$ and $t = 2$).

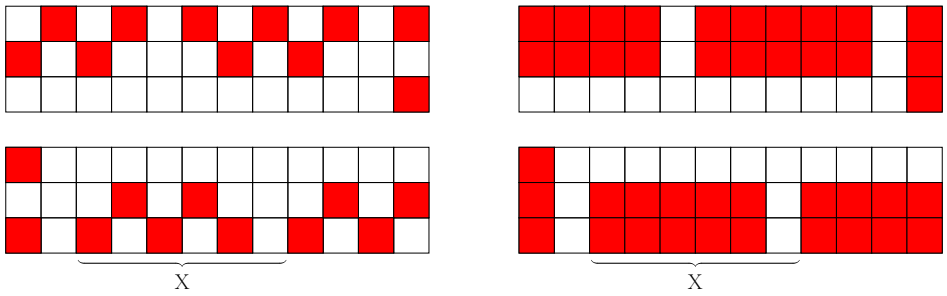


Figure 6.10: A perfect lethal set for $(3, 12, 2)$ with component $X$.

**Construction 6.6.** *All $(a, b, 2)$ grids with $a, b \in \{2, 5\} \pmod 6$, $a \neq b \pmod 6$, and $a, b > 2$ are perfect.*

*Proof.* Let $G$ be an $(a, b, 2)$ grid with $a, b \in \{2, 5\} \pmod 6$, $a \neq b \pmod 6$, and $a, b > 2$, and let $M$ be a manifold of $G$ and $H$ be its proper unfolding (Figure 6.11). Note that $M$ partitions the vertices of $V(G) \setminus M$ into two disjoint sets $R_1$ and $R_2$, both bounded by mutually orthogonal red, green, and blue faces. Note, also, that $H$ is obtained from $M$ by cutting along seams between red and green faces, and flattening the figure. Therefore, $H$ is a proper unfolding of $G$.

Let $X_1, \ldots, X_{k_1}$ be the repeated components of $H$ in the $x$-direction, and $Y_1, \ldots, Y_{k_2}$ be the repeated components of $H$ in the $y$-direction (see Figure 6.12). Denote by $X \times Y$ the union of these components. Let $A_t \subseteq V(H)$ be the set of infectious vertices in $H$ at time $t$, and suppose that for $i \in [k_1] \setminus \{1, k_1\}$ and $j \in [k_2]$, each $X_i \times Y_j$ contains the same pattern of infected vertices (see Figure 6.14). We show that $A_0$ is lethal and perfect.

Consider the initial infection $A_0$ of $H$ as shown in Figure 6.12. Observe that $A_0$ infects all vertices of $X \times Y$ by Proposition 2.7. We show that the remaining healthy vertices of $H$ become infected. The individual vertices in the rightmost column of $H$ are infected by Proposition 2.7. Consider re-folding $H$, and note that the two cells marked with an "X" in $H$ represent the same cell in $G$. This is enough to infect the remaining regions of $H$, and by Corollary 2.2, $A_0$ is lethal on $G$.

To prove that $A_0$ is perfect, observe that for $i \in [k_1] \setminus \{1\}$ and $j \in [k_2]$, each $X_i \times Y_j$ block contains exactly 12 infected vertices. For $j \in [k_2 - 1]$, $X_1 \times Y_j$ contains 11 infected vertices, and $X_1 \times Y_{k_2}$ contains 12 infected vertices. In total, the component $X \times Y$ contains exactly

$$12(k_1 - 1)(k_2) + 11(k_2 - 1) + 12$$

initially infected vertices. Of the remaining vertices in $H$, $14(k_1) - 1 + 9(k_2) + 8$ are

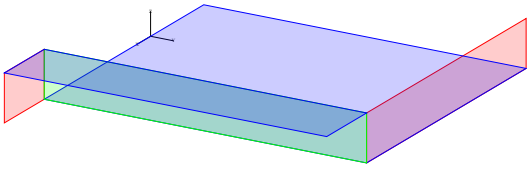

(a) A manifold of $G = (11, 20, 2)$.

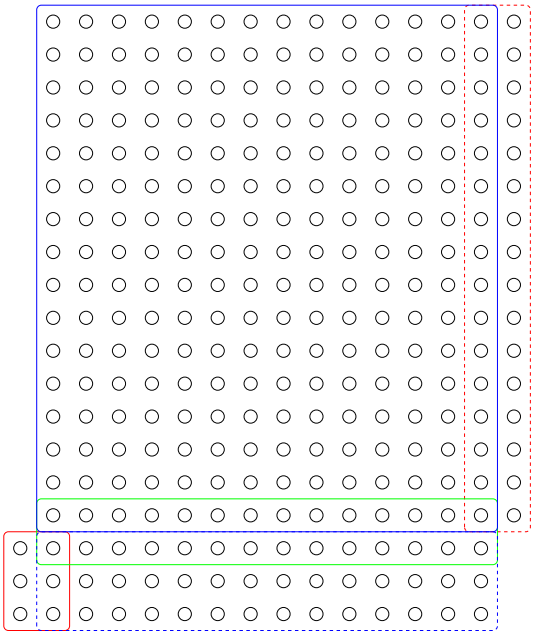

(b) A proper unfolding of $G$.

Figure 6.11: A proper unfolding of $G = (11, 20, 2)$. Colored rectangles indicate faces of $G$. Dashed lines indicate that cells appear on different layers.

infected. Therefore,

$$\begin{aligned} |A_0| &= 12(k_1 - 1)(k_2) + 11(k_2 - 1) + 12 + 14(k_1) - 1 + 9(k_2) + 8 \\ &= 12k_1k_2 + 14k_1 + 8k_2 + 8. \end{aligned}$$

The surface area bound for $G = (6k_1 + 2, 6k_2 + 5, 2)$ is given by

$$\begin{aligned} SA(6k_1 + 2, 6k_2 + 5, 2) &= \frac{(6k_1 + 2)(6k_2 + 5) + (6k_2 + 5)(2) + (2)(6k_1 + 2)}{3} \\ &= \frac{36(k_1)(k_2) + 42k_1 + 24k_2 + 24}{3} \\ &= 12k_1k_2 + 14k_1 + 8k_2 + 8. \end{aligned}$$

Since these two values are equal, $A_0$ is tight and lethal, and therefore perfect. □

**Construction 6.7.** *All $(a, b, 2)$ grids with $a, b \in \{0, 3\} \pmod 6$, $a \neq b \pmod 6$ and $a, b, \geq 6$ are perfect.*

*Proof.* Let $G$ be an $(a, b, 2)$ grid with $a, b \in \{0, 3\} \pmod 6$, $a \neq b \pmod 6$, and $a, b \geq 6$, and let $X_1, \ldots, X_{k_1}$ be the repeated components of $G$ in the $x$-direction, and $Y_1, \ldots, Y_{k_2}$ be the repeated components of $G$ in the $y$-direction (see Figure 6.15). Denote the union of these components by $X \times Y$. Let $A_t \subseteq V(H)$ be the set of infectious

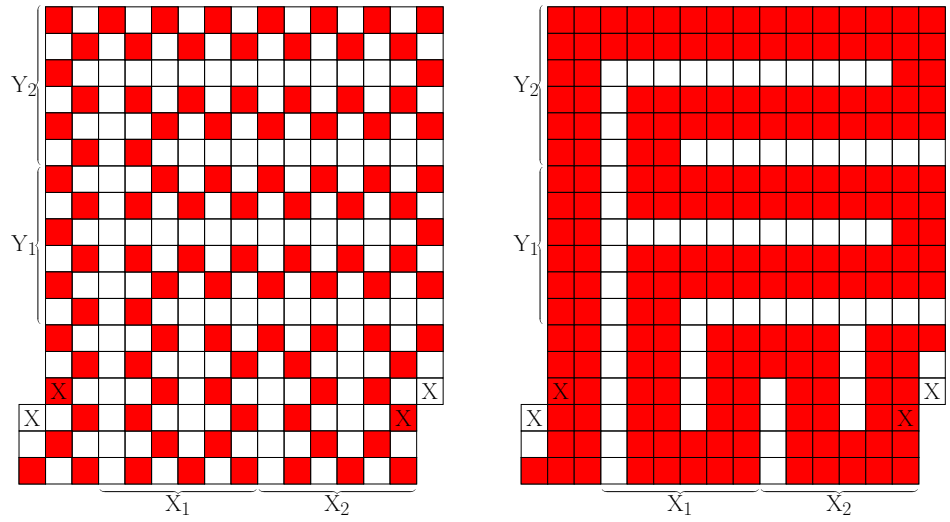


Figure 6.12: A percolating set on the proper unfolding of $G = (17, 14, 2)$.

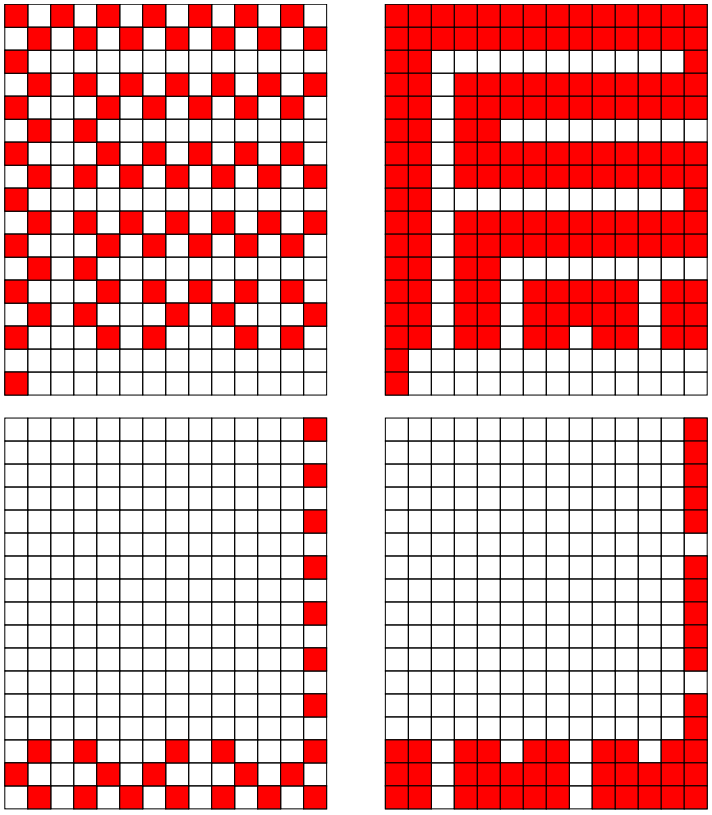

Figure 6.13: A perfect percolating set for $(17, 20, 2)$.

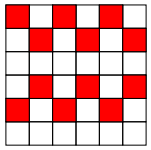

Figure 6.14: A block $X_i \times Y_j$.

vertices in $G$ at time $t$, and suppose that for $i \in [k_1]$ and $j \in [k_2]$, each $X_i \times Y_j$ contains the same pattern of infected vertices (see Figure 6.15). We show that $A_0$ is lethal and perfect.

Let $L_1$ and $L_2$ be the top and bottom layers of $G$, respectively. Observe that after one time-step, the subgraph of $L_1$ induced by the uninfected vertices of $\cup Y_i$ is both acyclic and contains no border-to-border paths. Therefore, by Proposition 2.7, $A_0$ is lethal in $(\cup Y_i) \cap L_1$.

Consider these observations in the context of $G$. Figure 6.16 shows that after 5 additional time-steps, the remaining healthy vertices in $L_1$ form two corridors, marked by red arrows. The vertices in the upper corridor are infected by Proposition 2.7, and those in the lower corridor are infected by Lemma 6.2. Therefore, all vertices of $L_1$ become infected. Furthermore, the infected vertices in $L_2$ form a lethal set under the 2-neighbor process, and so, by Lemma 6.2, we conclude that $A_0$ is lethal on $G$ under the 3-neighbor process.

To prove that $A_0$ is perfect, observe that for $i \in [k_1]$ and $j \in [k_2]$, each $X_i \times Y_j$ block contains exactly 12 infected vertices, and so the total number of infected vertices in $X \times Y$ is $12k_1k_2$.

Of the remaining vertices in $G$, $16k_1 + 22k_2 + 28$ are infected. Therefore,

$$|A_0| = 12k_1k_2 + 16k_1 + 22k_2 + 28.$$

The surface area bound for $G = (6k_1 + 9, 6k_2 + 6, 2)$ is given by

$$\begin{aligned} SA(6k_1 + 9, 6k_2 + 6, 2) &= \frac{(6k_1 + 9)(6k_2 + 6) + (6k_2 + 6)(2) + (2)(6k_1 + 9)}{3} \\ &= \frac{36k_1k_2 + 48k_1 + 66k_2 + 84}{3} \\ &= 12k_1k_2 + 16k_1 + 22k_2 + 28. \end{aligned}$$

Since these two values are equal, $A_0$ is tight and lethal, and therefore perfect. □

We note that it is possible to examine grids of the form described above using a folding argument, *if* they are at least as large as $(12, 21, 2)$. However, such a process omits an infinite number of smaller grids. Nevertheless, the construction is of interest, and the grid and corresponding unfolded net are given in Figures A.7, A.8 and A.9 in the Appendix.

## 6.4 Thickness 3

**Construction 6.8.** *All $(a, 3, 3)$ grids $G$ with $a \equiv 0 \pmod 2$ and $a > 2$ are perfect.*

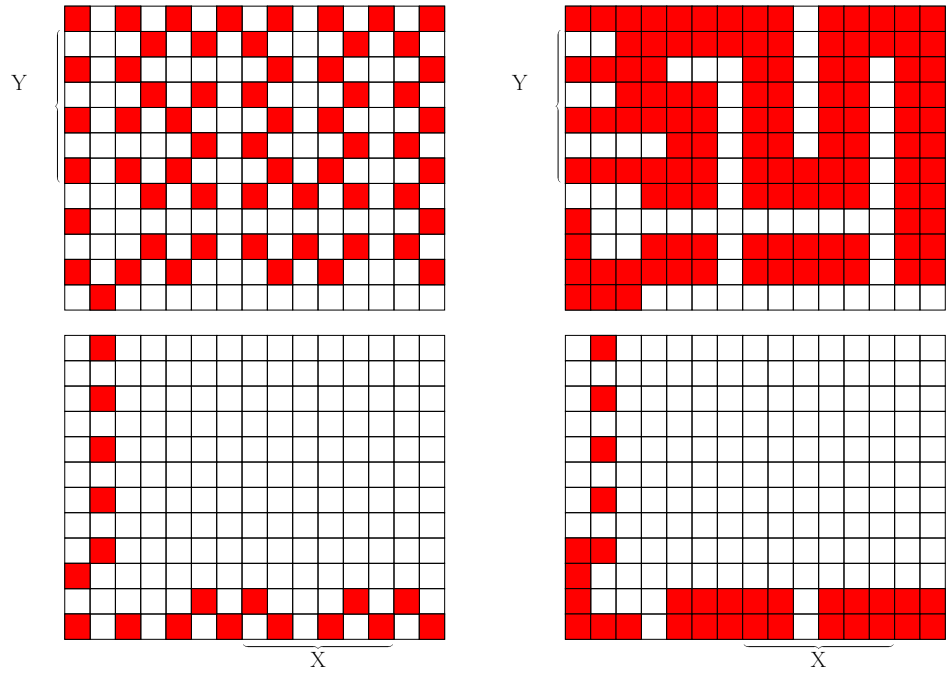


Figure 6.15: A perfect percolating set for $(12, 21, 2)$.

*Proof.* Let $G = (2k, 3, 3)$ be a grid such that $k > 1$. Let $A = \{1, 2, 3\} \times [3] \times [3]$, $B = \{2k\} \times [3] \times [3]$, and $X_i = \{2i+2, 2i+3\} \times [3] \times [3]$ for $i \in [k-2]$, be components of $G$. Denote by $AX^kB$ the union of components $A \cup X_1 \cup \cdots \cup X_k \cup B$, and note that $G = AX^kB$. Let $A_t^k \subseteq V(G)$ be the set of infectious vertices in $G$ at time $t$, and suppose that each $X_i$ contains the same pattern of infected vertices (see Figure 6.17). We show that $A_0^k$ is lethal and perfect.

Consider the union of components $AX^k = A \cup X_1 \cup \cdots \cup X_k$ (see Figure 6.18). Let $L_1$, $L_2$ and $L_3$ be the top, middle and bottom levels of $AX^k$, respectively. Observe that after one time-step, the subgraph of $L_2 \setminus \{2k-1\} \times [3] \times \{2\}$ induced by $\overline{A_0^k}$ is acyclic with no border-to-border vertices, and so by Proposition 2.7, $A_0^k$ infects all vertices of $L_2$ apart from those in the rightmost column (labeled "X"; see Figure 6.18). Therefore, by Lemma 6.2, all vertices in $L_1$ apart from the rightmost column (labeled "Y") become infected by the 2-neighbor process. Similarly, the red arrow in Figure 6.18) shows the path of infection in $L_3$.

Consider these observations in the context of $G$. Figure 6.19 shows that it takes 7 additional time-steps to fully infect $L_1$ and $L_2$. By Lemma 6.2, the remaining healthy vertices in $L_3$ become infected. We therefore conclude that $A_0^k$ is lethal on $G$ under the 3-neighbor process.

To prove that $A_0^k$ is perfect, observe that $|A_0^k| = 8 + 4(k-2) + 3 = 4k + 3$. The

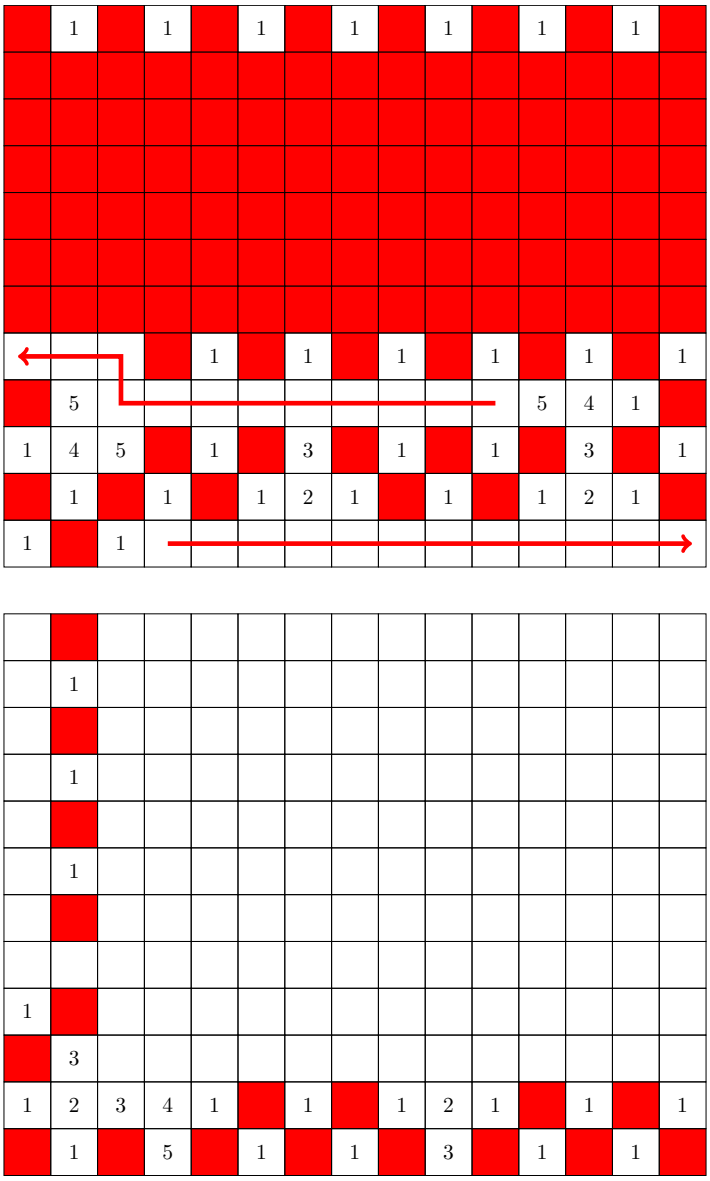


Figure 6.16: A perfect percolating set for $(12, 21, 2)$.

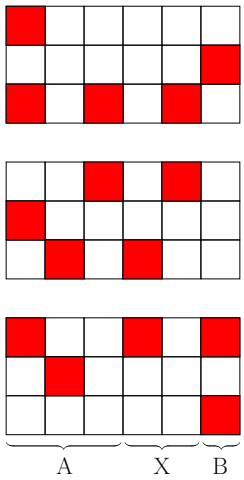


Figure 6.17: The components $A$, $X$, $B$ on $G = AXB$ with infectious set $A_0$.

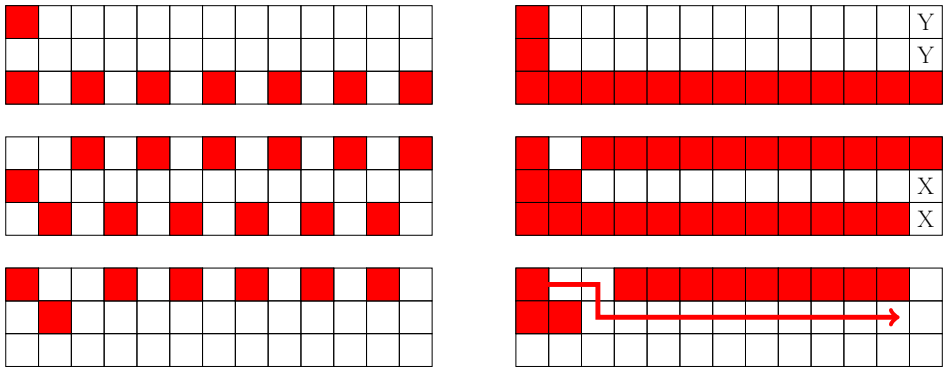


Figure 6.18: An infection on $AX^5$, $t = 0$ and $t = 1$.

surface area bound for $G = (2k, 3, 3)$ is given by

$$\frac{(2k)(3) + (3)(3) + (3)(2k)}{3} = \frac{12k + 9}{3} = 4k + 3.$$

Since these two values are equal, $A_0^k$ is tight and lethal, and therefore perfect. □

**Construction 6.9.** *All* $(a, b, 3)$ *grids* $G$ *with* $a \equiv 3 \pmod 6$, $b \equiv 1 \pmod 2$ *and* $a, b \geq 3$ *are perfect.*

*Proof.* Consider the grid $H = (a+2, b+2, 1)$, where $a \equiv 3 \pmod 6$ and $b \equiv 1 \pmod 2$. Observe that $H$ admits an optimal percolating set by Construction 6.3, and that

$$\mathrm{SA}(a, b, 3) = \lceil \mathrm{SA}(a + 2, b + 2, 1) \rceil - 3.$$

We show that a proper unfolding of $G$ can be obtained from a simple augmentation of $H$. Let $H'$ be the grid obtained by deleting the four vertices in the bottom, right-most

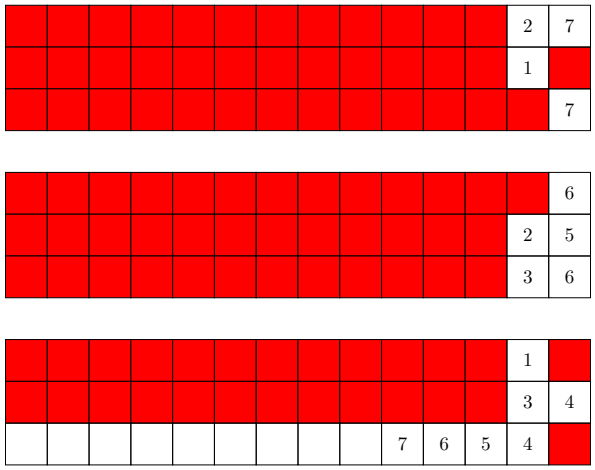


Figure 6.19: An infection on $G$.

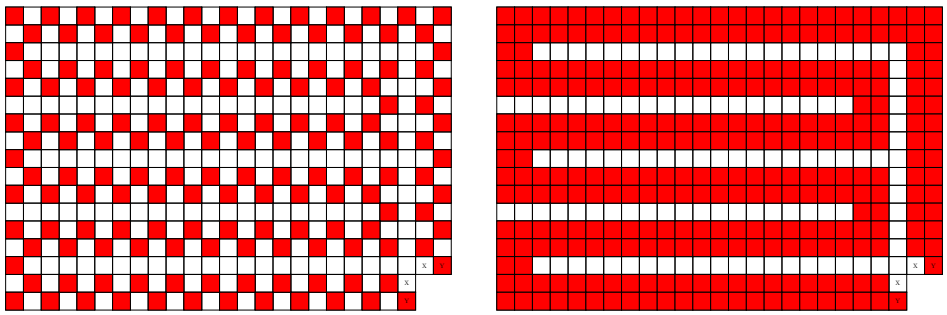

Figure 6.20: A percolating set on the proper unfolding $H'$ of $G = (15, 23, 3)$.

corner of $H$ (see Figure 6.20). Consider the folding pattern illustrated in Figure 6.21, and observe that the pairs of vertices adjacent to the deleted region are duplicates of each other. (In other words, consider folding up the red and green regions in Figure 6.21, and notice that this operation causes vertices to overlap.) Taking this into account, $H'$ percolates by Proposition 2.7. Since $H$ admits an optimal percolating set of size $\lceil \mathrm{SA}(a+2, b+2, 1) \rceil$, and precisely 3 of the vertices deleted from $H$ to obtain $H'$ were infected, it follows that $H'$ admits a perfect lethal set. Finally, by Lemma 2.2, $G$ is perfect. □

**Construction 6.10.** *All* $(a, 4, 3)$ *grids* $G$ *with* $a \equiv 3 \pmod 6$ *and* $a \geq 9$ *are perfect.*

*Proof.* Let $G = (6k+3, 4, 3)$ be a grid such that $k \geq 1$, and let $X_1, \ldots, X_k$ be the repeated components of $G$ in the $x$-direction. Denote the union of these components by $X^k$. Let $A_t^k \subseteq V(G)$ be the set of infectious vertices in $G$ at time $t$, and suppose that each $X_i$ contains the same pattern of infected vertices (see Figure 6.22). We show that $A_0^k$ is lethal and perfect.

Let $L_1$, $L_2$ and $L_3$ be the top, middle and bottom levels of $G$, respectively. Consider $L_3$ at $t = 1$ (see Figure 6.22). Observe that the vertices labeled "X" are infected at

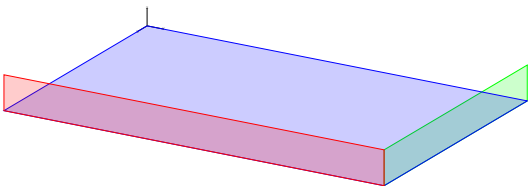

(a) A manifold of $G = (15, 23, 3)$.

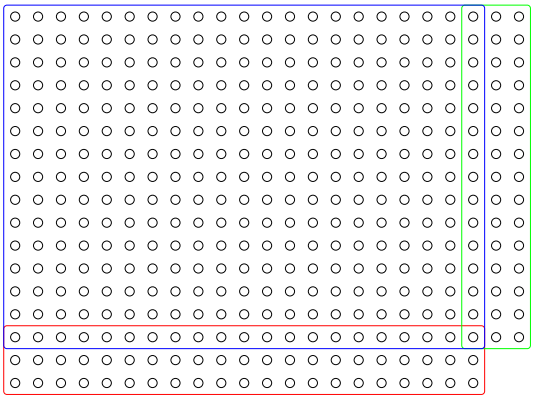

(b) A proper unfolding of $G$.

Figure 6.21: A proper unfolding of $G = (15, 23, 3)$. Colored rectangles indicate faces of $G$.

$t = 2$, and subsequently all vertices in $X^k \cap L_3$ (with the exception of the vertex labeled "Y") are infected by Proposition 2.7. Additionally, the infected vertices in $L_2$ at $t = 1$ are lethal in $X^k \cap L_2$ under the 2-neighbor process, and so by Lemma 6.2, all vertices of $X^k \cap L_2$ (apart from the one labeled "Y") are infected.

Consider these observations in the context of $G$. Figure 6.23 shows that it takes 5 additional time-steps to fully infect $L_2$. By Lemma 6.2, the remaining healthy vertices in $L_1$ and $L_3$ become infected. We therefore conclude that $A_0^k$ is lethal on $G$ under the 3-neighbor process.

To prove that $A_0^k$ is perfect, observe that for $i \in [k]$, each $X_i$ contains 14 infected vertices. Of the remaining vertices in $G$, 11 are infected. Therefore, $|A_0| = 14k + 11$. The surface area bound for $G = (6k + 3, 4, 3)$ is given by

$$\frac{(6k+3)(4) + (4)(3) + (3)(6k+3)}{3} = \frac{42k + 33}{3} = 14k + 11.$$

Since these two values are equal, $A_0^k$ is tight and lethal, and therefore perfect. □

**Construction 6.11.** *All $(a, 6, 3)$ grids $G$ with $a \equiv 0 \pmod 2$ and $a \geq 4$ are perfect.*

*Proof.* Let $G = (2k + 2, 6, 3)$ be a grid such that $k \geq 1$, and let $X_1, \ldots, X_k$ be the repeated components of $G$ in the $x$-direction. Denote the union of these components by $X^k$. Let $A_t^k \subseteq V(G)$ be the set of infectious vertices in $G$ at time $t$, and suppose that each $X_i$ contains the same pattern of infected vertices (see Figure 6.24). We show that $A_0^k$ is lethal and perfect.

Let $L_1$, $L_2$ and $L_3$ be the top, middle and bottom levels of $G$, respectively. Consider $L_2$ at $t = 1$ (see Figure 6.24). Observe that all vertices in $X^k \cap L_2$ are infected by Proposition **??**, due to adjacent infected vertices in $L_1$ and$L_3$.

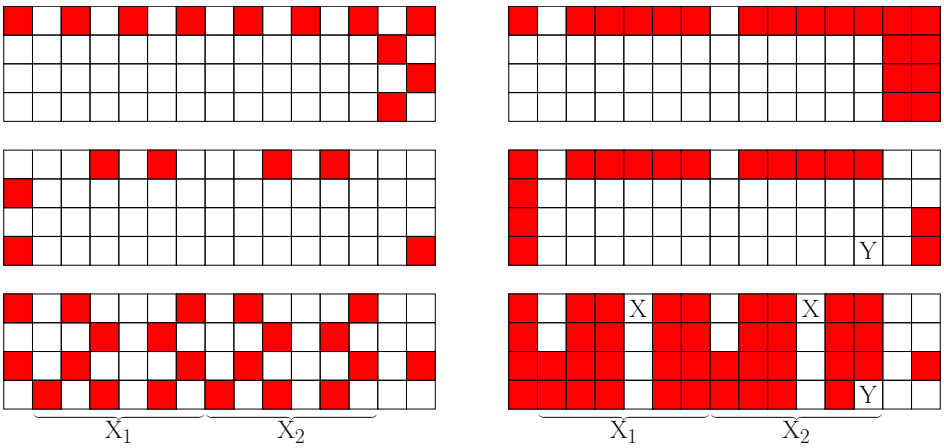


Figure 6.22: A lethal set on $(4, 15, 3)$, $t = 0$ and $t = 1$.

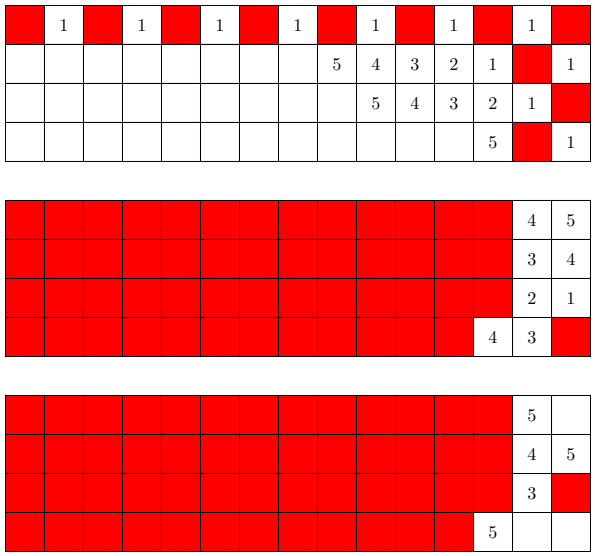


Figure 6.23: A lethal set on $(4, 15, 3)$, $t = 0$ and $t = 1$.

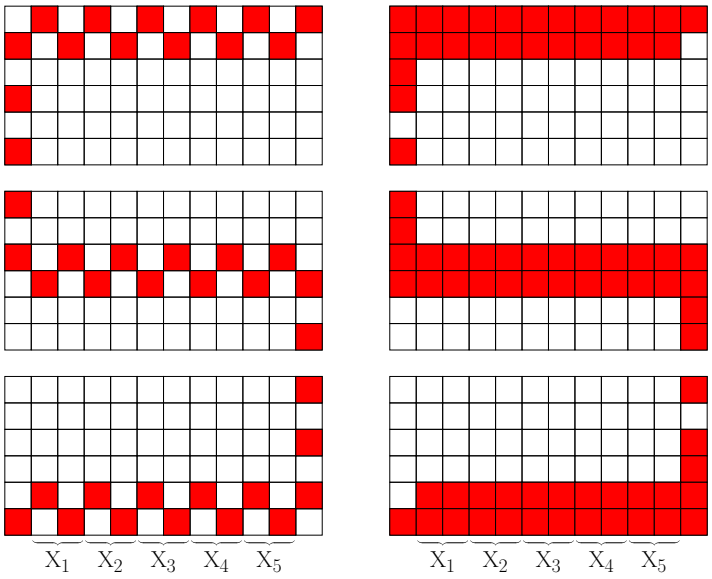


Figure 6.24: A lethal set on $(6, 12, 3)$, $t = 0$ and $t = 1$.

Consider these observations in the context of $G$. Figure 6.25 shows that it takes 2 additional time-steps to fully infect $L_2$. Since $L_1$ and $L_3$ contain lethal sets under the 2-neighbor process, by Lemma 6.2, the remaining healthy vertices in these levels become infected. We therefore conclude that $A_0^k$ is lethal on $G$ under the 3-neighbor process.

To prove that $A_0^k$ is perfect, observe that for $i \in [k]$, each $X_i$ contains 6 infected vertices. Of the remaining vertices in $G$, 12 are infected. Therefore, $|A_0| = 6k + 12$. The surface area bound for $G = (2k + 2, 6, 3)$ is given by

$$\frac{(2k+2)(6) + (6)(3) + (3)(2k+2)}{3} = \frac{18k + 36}{3} = 6k + 12.$$

Since these two values are equal, $A_0^k$ is tight and lethal, and therefore perfect. □

**Construction 6.12.** *All $(a, 6, 3)$ grids $G$ with $a \equiv 1 \pmod 2$ and $a \geq 5$ are perfect.*

*Proof.* Let $G = (2k + 3, 6, 3)$ be a grid such that $k \geq 1$, and let $X_1, \ldots, X_k$ be the repeated components of $G$ in the $x$-direction. Denote the union of these components by $X^k$. Let $A_t^k \subseteq V(G)$ be the set of infectious vertices in $G$ at time $t$, and suppose that each $X_i$ contains the same pattern of infected vertices (see Figure 6.26a). We show that $A_0^k$ is lethal and perfect.

Let $L_1$, $L_2$ and $L_3$ be the top, middle and bottom levels of $G$, respectively. Consider $L_2$ at $t = 1$ (see Figure 6.26a). Observe that all vertices in $X^k \cap L_2$ (with the exception of the one labeled "X") are infected by Proposition **??**, due to adjacent infected vertices in $L_1$ and$L_3$.

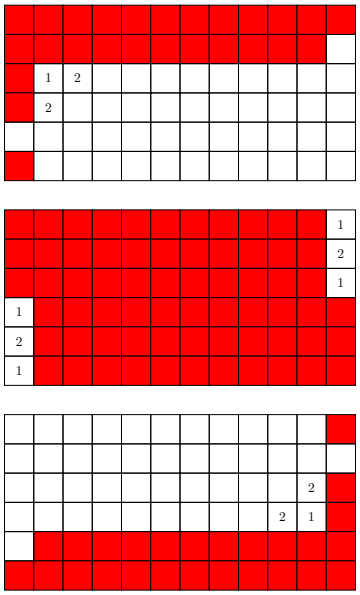

Figure 6.25: Timesteps to infect $L_2$.

Consider these observations in the context of $G$. Figure 6.26b shows that it takes 5 additional time-steps to fully infect $L_2$. Since $L_1$ and $L_3$ contain lethal sets under the 2-neighbor process, by Lemma 6.2, the remaining healthy vertices in these levels become infected. We therefore conclude that $A_0^k$ is lethal on $G$ under the 3-neighbor process.

To prove that $A_0^k$ is perfect, observe that for $i \in [k]$, each $X_i$ contains 6 infected vertices. Of the remaining vertices in $G$, 15 are infected. Therefore, $|A_0| = 6k + 15$. The surface area bound for $G = (2k + 3, 6, 3)$ is given by

$$\frac{(2k+3)(6) + (6)(3) + (3)(2k+3)}{3} = \frac{18k + 45}{3} = 6k + 15.$$

Since these two values are equal, $A_0^k$ is tight and lethal, and therefore perfect. □

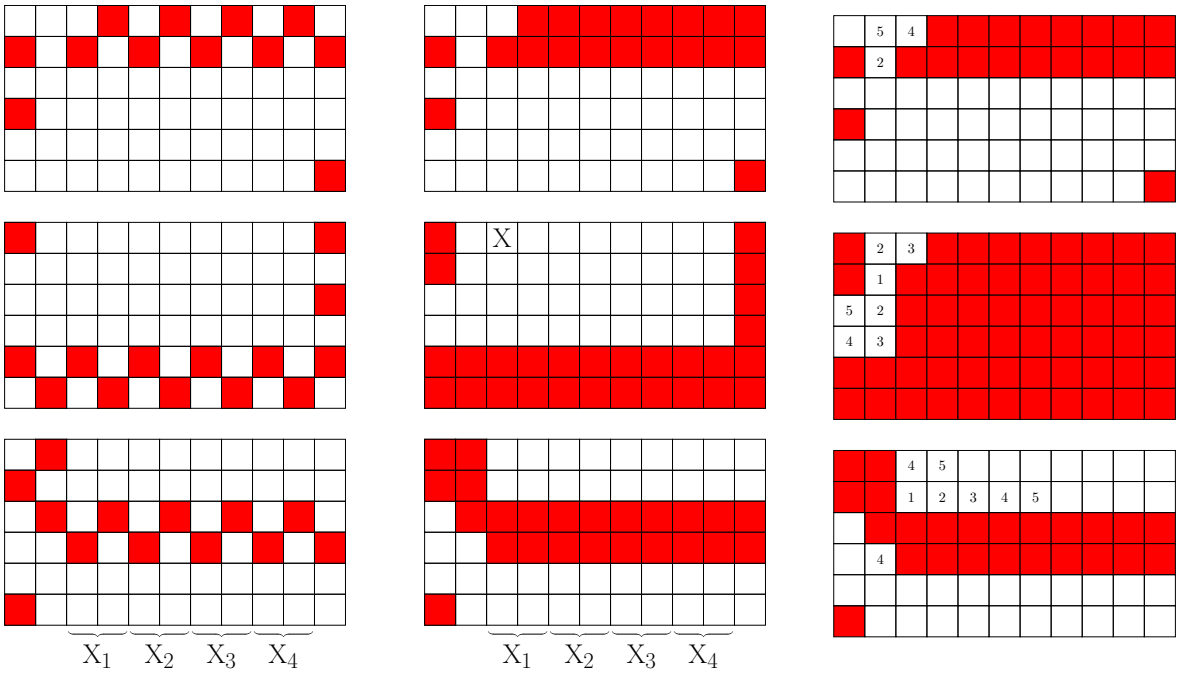


(a) A lethal set on $(6, 11, 3)$, $t = 0$ and $t = 1$.

(b) Timesteps to infect $L_2$.

Figure 6.26

# Chapter 7
# Conclusion

# Appendix A
# Individual Constructions

We diagram lethal set constructions for single grids. The initial infection $A$ is colored red, and all other cells are labeled with the time $t$ that they are first infected.

## A.1 Perfect constructions

**Construction A.1.** *The grid* $(3, 3, 1)$ *is perfect.*

*Proof.* See Figure A.1. □

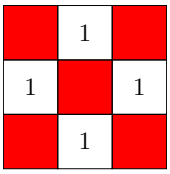


Figure A.1

**Construction A.2.** *The grid* $(5, 2, 2)$ *is perfect.*

*Proof.* See Figure A.2. □

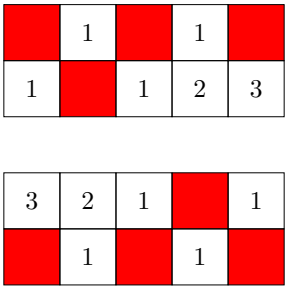


Figure A.2

**Construction A.3.** *The grid* $(5, 5, 2)$ *is perfect.*

*Proof.* See Figure A.3. □

| | | | | |
|---|---|---|---|---|
| | 1 | | 1 | |
| 1 | | 1 | 2 | 1 |
| | 1 | | 3 | |
| 1 | 2 | 1 | 4 | 5 |
| | 3 | | 1 | |

| | | | | |
|---|---|---|---|---|
| 11 | 10 | 9 | | 1 |
| 10 | 9 | 8 | 3 | |
| 9 | 8 | 7 | 6 | 7 |
| | 3 | | 5 | 8 |
| 5 | 4 | 1 | | 9 |

Figure A.3

**Construction A.4.** *The grid* $(6, 4, 3)$ *is perfect.*

*Proof.* See Figure A.4. □

| | | | | | |
|---|---|---|---|---|---|
| 8 | 1 | | 11 | 14 | 15 |
| 7 | | 1 | | 13 | |
| | 1 | 6 | 7 | 14 | 15 |
| 1 | | 9 | 10 | 17 | 18 |

| | | | | | |
|---|---|---|---|---|---|
| 7 | | 1 | 10 | 11 | |
| 6 | 3 | 4 | 5 | 12 | 1 |
| 1 | 2 | 5 | | 13 | |
| | 1 | 8 | 9 | 16 | 17 |

| | | | | | |
|---|---|---|---|---|---|
| | 1 | | 9 | | 17 |
| 5 | 4 | 5 | 8 | 13 | 16 |
| | 3 | 6 | 7 | 14 | 15 |
| 1 | | 7 | | 15 | |

Figure A.4

**Construction A.5.** *The grid* $(8, 5, 5)$ *is perfect.*

*Proof.* See Figure A.5. □

| | | | | | | | |
|---|---|---|---|---|---|---|---|
| | 1 | | 33 | 34 | 35 | 36 | 37 |
| 37 | 30 | 23 | 22 | 21 | 20 | 19 | |
| 38 | 31 | 10 | 9 | | 9 | 16 | 17 |
| 39 | 32 | 9 | 8 | 7 | 8 | 15 | 18 |
| 40 | 33 | | 1 | | 1 | | 19 |

| | | | | | | | |
|---|---|---|---|---|---|---|---|
| 1 | | 25 | 32 | 33 | 34 | 35 | |
| 36 | 29 | 24 | 21 | 20 | 19 | 18 | 17 |
| 37 | 30 | 9 | 8 | 7 | | 15 | 16 |
| 38 | 31 | 8 | 7 | 6 | 5 | 14 | 15 |
| 39 | 32 | 7 | | 1 | | 1 | |

| | | | | | | | |
|---|---|---|---|---|---|---|---|
| | 29 | 30 | 31 | 32 | 33 | 36 | 37 |
| 35 | 28 | 25 | | 13 | 14 | 15 | 18 |
| 36 | 9 | | 1 | 8 | 9 | 14 | 15 |
| 37 | 8 | 5 | | 3 | 4 | 13 | |
| | 7 | 6 | 1 | 2 | 3 | 14 | 15 |

| | | | | | | | |
|---|---|---|---|---|---|---|---|
| 33 | 32 | 31 | | 13 | | 37 | 38 |
| 34 | 27 | 26 | 1 | 12 | 11 | | 19 |
| 35 | | 3 | 2 | 9 | 10 | 11 | |
| 38 | 5 | 4 | 1 | | 1 | 12 | 1 |
| 39 | | 1 | | 1 | | 15 | 16 |

| | | | | | | | |
|---|---|---|---|---|---|---|---|
| | 33 | 34 | 35 | 36 | 37 | 38 | 39 |
| 1 | | 27 | | 33 | 34 | 35 | 36 |
| | 1 | 28 | 29 | 32 | 33 | 34 | 35 |
| 39 | 30 | 29 | 30 | 31 | | 13 | |
| 40 | 31 | | 31 | 32 | 33 | 34 | 35 |

Figure A.5

**Construction A.6.** *The grid* $(9, 6, 5)$ *is perfect.*

*Proof.* See Figure A.6. □

| | | | | | | | | |
|---|---|---|---|---|---|---|---|---|
| 38 | 37 | | 31 | 32 | 33 | 34 | 35 | |
| 11 | 10 | 7 | | 11 | 24 | 25 | 28 | 29 |
| | 7 | 6 | 1 | | 23 | 24 | 27 | 28 |
| 9 | 8 | 3 | | 1 | 22 | 23 | 26 | 27 |
| 26 | 9 | | 19 | 20 | 21 | 22 | 23 | |
| 39 | 38 | 37 | 36 | 35 | | 1 | | 1 |

| | | | | | | | | |
|---|---|---|---|---|---|---|---|---|
| 37 | 36 | 29 | 30 | 31 | 32 | 33 | 36 | 37 |
| | 9 | 8 | 5 | 10 | 15 | 20 | 27 | 30 |
| 1 | 6 | 5 | 4 | 1 | | 19 | 26 | 27 |
| | 1 | 2 | 3 | | 1 | | 25 | 26 |
| 25 | | 1 | 18 | 17 | 16 | 1 | 24 | 25 |
| 34 | 33 | | 33 | 34 | 17 | | 1 | |

| | | | | | | | | |
|---|---|---|---|---|---|---|---|---|
| 36 | 35 | 28 | 27 | | 15 | 20 | 37 | 38 |
| 11 | 10 | 9 | | 9 | 14 | 19 | 20 | 31 |
| 8 | 7 | | 5 | 8 | 13 | 18 | 19 | |
| 1 | | 1 | 6 | 7 | 14 | 15 | 20 | 21 |
| 24 | 21 | 20 | 19 | | 15 | | 25 | 26 |
| 33 | 32 | 31 | 32 | 35 | 36 | 37 | 38 | 39 |

| | | | | | | | | |
|---|---|---|---|---|---|---|---|---|
| 35 | 34 | 27 | 26 | 1 | | 19 | 38 | 39 |
| 22 | 21 | 20 | 19 | 10 | 11 | 18 | 19 | 32 |
| 21 | 20 | 19 | 18 | 11 | 12 | 17 | 18 | 1 |
| | 1 | | 17 | 16 | 15 | 16 | 19 | |
| 23 | 22 | 21 | 20 | 19 | 18 | 17 | 26 | 27 |
| | 23 | 30 | 31 | 36 | 37 | 38 | 39 | 40 |

| | | | | | | | | |
|---|---|---|---|---|---|---|---|---|
| | 33 | | 25 | | 1 | | 39 | 40 |
| 33 | 32 | 25 | 24 | 3 | 2 | 1 | | 33 |
| 34 | 31 | 26 | 23 | | 1 | | 1 | |
| 35 | 30 | 27 | 22 | 17 | | 1 | 20 | 21 |
| 36 | 29 | 28 | 21 | 20 | 19 | | 27 | 28 |
| 37 | | 29 | | 37 | 38 | 39 | 40 | 41 |

Figure A.6

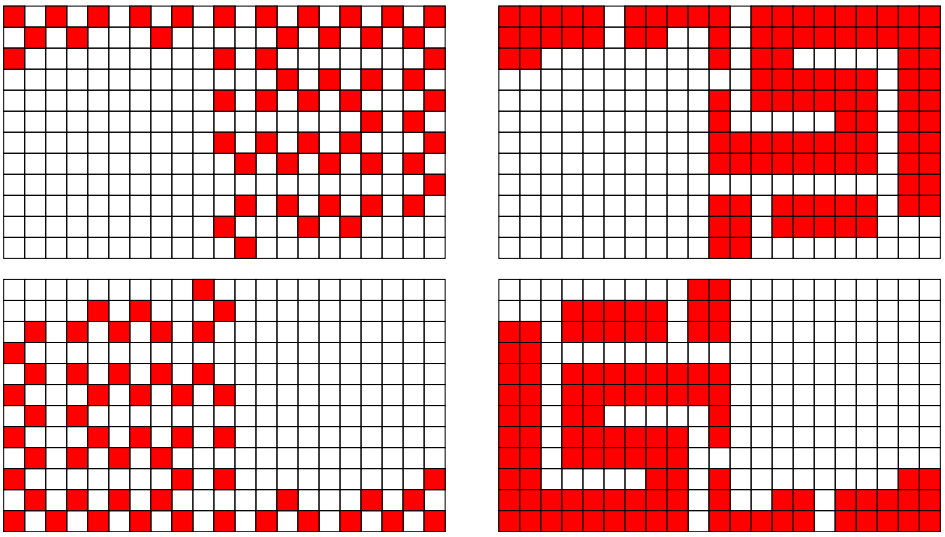

Figure A.7: A perfect percolating set for $(12, 21, 2)$.

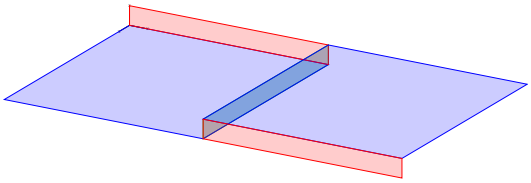

(a) A manifold of $G = (12, 21, 2)$.

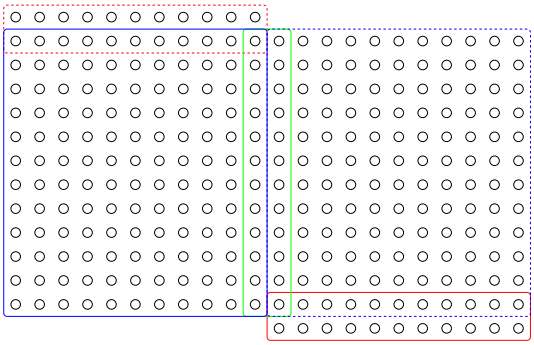

(b) A proper unfolding of $G$.

Figure A.8: A proper unfolding of $G = (12, 21, 2)$. Colored rectangles indicate faces of $G$. Dashed lines indicate that cells appear on different layers.

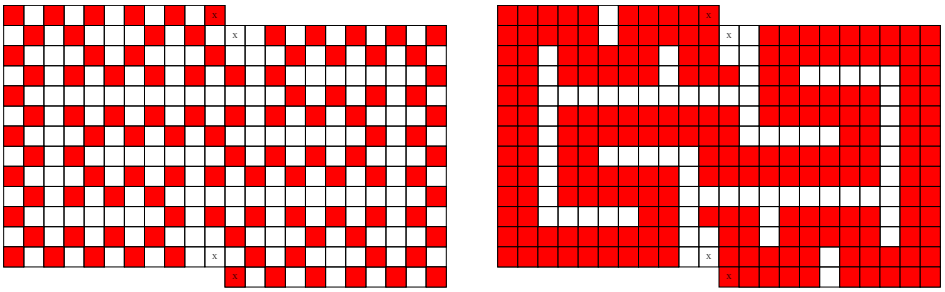

Figure A.9: A percolating set on the proper unfolding of $G = (12, 21, 2)$.

## A.2 Optimal constructions

**Construction A.7.** *The grid* $(6, 5, 5)$ *is optimal.*

*Proof.* See Figure A.10. □

| | | | | | |
|---|---|---|---|---|---|
| | 29 | 26 | 25 | | 1 |
| 31 | 30 | 11 | 8 | 1 | |
| 32 | 31 | | 1 | | 1 |
| 33 | 32 | 1 | | 1 | |
| 34 | 33 | | 1 | | 1 |

| | | | | | |
|---|---|---|---|---|---|
| 29 | 28 | 25 | 24 | 3 | |
| 30 | 27 | 10 | 7 | 2 | 1 |
| 31 | 10 | 7 | 6 | 1 | |
| 32 | 7 | 6 | 5 | 2 | 1 |
| 33 | | 1 | 4 | 3 | |

| | | | | | |
|---|---|---|---|---|---|
| | 27 | 24 | 23 | 16 | 15 |
| 27 | 26 | 9 | | 3 | 14 |
| | 9 | 8 | 7 | | 13 |
| 29 | | 7 | 8 | 9 | 12 |
| 30 | 1 | | 9 | 10 | 11 |

| | | | | | |
|---|---|---|---|---|---|
| 29 | 28 | 23 | 22 | 17 | |
| 28 | 25 | | 19 | 18 | 15 |
| 25 | 24 | 21 | 20 | 19 | 16 |
| 28 | 25 | 22 | 21 | 20 | 13 |
| 29 | 26 | 23 | 22 | 21 | |

| | | | | | |
|---|---|---|---|---|---|
| 30 | 29 | | 21 | | 1 |
| 29 | | 1 | 20 | 19 | |
| | 23 | 22 | 21 | 20 | 17 |
| 27 | 26 | 23 | 22 | 21 | |
| | 27 | 28 | 29 | 30 | 31 |

Figure A.10

**Construction A.8.** *The grid* $(7, 5, 5)$ *is optimal.*

*Proof.* See Figure A.11. □

| | | | | | | |
|---|---|---|---|---|---|---|
| 28 | 27 | 12 | 1 | | 1 | |
| 27 | 26 | 11 | | 1 | 2 | 1 |
| 26 | 25 | | 1 | | 3 | |
| 25 | 24 | 23 | 24 | 25 | 26 | 27 |
| | 1 | | 25 | 26 | 27 | 28 |

| | | | | | | |
|---|---|---|---|---|---|---|
| 19 | 16 | 11 | | 1 | | 1 |
| 18 | 15 | 10 | 5 | 4 | 3 | |
| 17 | 14 | 7 | 6 | 5 | 6 | 7 |
| | 1 | 22 | 23 | 24 | 25 | 26 |
| 1 | | 23 | 24 | 25 | 26 | 27 |

| | | | | | | |
|---|---|---|---|---|---|---|
| | 15 | | 1 | 10 | 11 | |
| 15 | 14 | 9 | 8 | 9 | 12 | 13 |
| 16 | 13 | | 7 | | 13 | 14 |
| 17 | | 21 | 20 | 19 | 16 | 15 |
| 26 | 25 | 24 | 21 | 20 | 17 | |

| | | | | | | |
|---|---|---|---|---|---|---|
| 17 | 16 | 1 | | 19 | 20 | 21 |
| | 11 | 10 | 11 | 18 | 19 | 20 |
| 13 | 12 | 11 | 12 | 17 | 16 | 15 |
| 24 | 23 | 22 | 19 | 18 | 1 | |
| 27 | 26 | 25 | | 1 | | 1 |

| | | | | | | |
|---|---|---|---|---|---|---|
| 18 | 17 | | 23 | 24 | 25 | 26 |
| 1 | | 1 | 22 | 23 | 24 | 25 |
| | 1 | | 21 | 20 | 17 | |
| 25 | 24 | 23 | 22 | 19 | | 1 |
| 28 | 27 | 26 | 23 | | 1 | 2 |

Figure A.11

**Construction A.9.** *The grid* $(7, 6, 5)$ *is optimal.*

*Proof.* See Figure A.12. □

| | | | | | | |
|---|---|---|---|---|---|---|
| 34 | 33 | 32 | 1 | | 3 | |
| 33 | 32 | 25 | | 1 | 2 | 1 |
| 32 | 31 | 24 | 21 | | 1 | |
| 25 | 24 | 23 | 22 | 23 | 24 | 25 |
| | 1 | | 7 | 24 | 25 | 26 |
| 1 | | 1 | | 25 | 26 | 27 |

| | | | | | | |
|---|---|---|---|---|---|---|
| 33 | 32 | 31 | | 21 | 22 | 23 |
| 32 | 31 | 24 | 21 | 20 | 3 | |
| 31 | 30 | 21 | 20 | 19 | | 1 |
| | 3 | | 7 | 20 | 21 | 22 |
| 1 | 2 | 1 | 6 | 21 | 22 | 23 |
| | 3 | 4 | 5 | 22 | 23 | 24 |

| | | | | | | |
|---|---|---|---|---|---|---|
| | 29 | 30 | 31 | 32 | 33 | 34 |
| 1 | | 23 | 22 | 21 | 20 | 19 |
| 30 | 29 | | 19 | 18 | 17 | 18 |
| 31 | 30 | 1 | 2 | 1 | | 19 |
| 32 | 31 | | 1 | | 11 | 20 |
| 33 | 32 | 5 | | 9 | 12 | 21 |

| | | | | | | |
|---|---|---|---|---|---|---|
| 1 | 28 | 29 | 32 | 33 | 34 | 35 |
| | 25 | 24 | 23 | 22 | 21 | |
| 29 | 28 | 21 | 20 | 17 | 16 | 15 |
| 32 | 31 | 6 | 3 | | 11 | 14 |
| 33 | 32 | 5 | 4 | 5 | 10 | 11 |
| 34 | 33 | 6 | 5 | 8 | 9 | |

| | | | | | | |
|---|---|---|---|---|---|---|
| | 27 | | 33 | 34 | 35 | 36 |
| 1 | 26 | 25 | 26 | 27 | 28 | 29 |
| | 27 | 22 | 21 | | 13 | |
| 33 | 32 | 7 | | 1 | 12 | 13 |
| 34 | 33 | | 1 | 6 | 7 | |
| 35 | 34 | 7 | | 7 | | 1 |

Figure A.12

**Construction A.10.** *The grid* $(7, 7, 5)$ *is optimal.*

*Proof.* See Figure A.13. □

| | | | | | | |
|---|---|---|---|---|---|---|
| 24 | 23 | 22 | 1 | | 1 | |
| 21 | 20 | 17 | | 1 | 2 | 1 |
| 20 | 19 | 10 | 9 | | 3 | |
| 1 | | 7 | 10 | 11 | 18 | 19 |
| | 1 | | 11 | 12 | 19 | 20 |
| 1 | 2 | 3 | 18 | 19 | 20 | 21 |
| | 1 | | 19 | 20 | 21 | 22 |

| | | | | | | |
|---|---|---|---|---|---|---|
| 23 | 22 | 21 | | 1 | | 1 |
| 20 | 19 | 16 | 5 | 4 | 3 | |
| 19 | 18 | 9 | 8 | 5 | 6 | 7 |
| | 5 | 6 | 7 | | 17 | 18 |
| 1 | 4 | 5 | 8 | 9 | 18 | 19 |
| | 3 | 6 | 17 | 18 | 19 | 20 |
| 1 | | 7 | 18 | 19 | 20 | 21 |

| | | | | | | |
|---|---|---|---|---|---|---|
| | 19 | 20 | 21 | 22 | 23 | 24 |
| 19 | 18 | 15 | 12 | 11 | 18 | 19 |
| | 17 | | 9 | 10 | 17 | 18 |
| 19 | 18 | 1 | | 1 | 16 | 17 |
| 20 | 19 | | 1 | | 15 | |
| 21 | 20 | 17 | 16 | 15 | 16 | 17 |
| 22 | 21 | 18 | 17 | | 17 | 18 |

| | | | | | | |
|---|---|---|---|---|---|---|
| 21 | | 15 | 22 | 23 | 24 | 25 |
| 20 | 15 | 14 | 13 | | 19 | 20 |
| 17 | 16 | 13 | 12 | 11 | 18 | 19 |
| 20 | 19 | 14 | 13 | 12 | 15 | |
| 21 | 20 | 15 | 14 | 13 | 14 | 1 |
| 22 | 21 | 18 | 15 | 14 | 15 | 16 |
| 23 | 22 | 19 | | 1 | 16 | 17 |

| | | | | | | |
|---|---|---|---|---|---|---|
| 22 | 1 | | 23 | 24 | 25 | 26 |
| 21 | | 1 | 14 | 15 | 20 | 21 |
| | 1 | | 1 | | 19 | 20 |
| 21 | 20 | 15 | | 1 | 16 | 17 |
| 22 | 21 | 16 | 15 | | 1 | |
| 23 | 22 | 19 | 16 | 1 | | 1 |
| 24 | 23 | 20 | 17 | | 1 | |

Figure A.13

# Bibliography


[1] J. Balogh and B. Bollobás. Bootstrap percolation on the hypercube. *Probability Theory and Related Fields*, 134(4):624–648, 2006.

[2] F. Benevides, J.-C. Bermond, H. Lesfari, and N. Nisse. *Minimum lethal sets in grids and tori under 3-neighbour bootstrap percolation.* PhD thesis, Université Côte d'Azur, 2021.

[3] F. Benevides and M. Przykucki. On slowly percolating sets of minimal size in bootstrap percolation. *the electronic journal of combinatorics*, pages P46–P46, 2013.

[4] F. Benevides and M. Przykucki. Maximum percolation time in two-dimensional bootstrap percolation. *SIAM Journal on Discrete Mathematics*, 29(1):224–251, 2015.

[5] B. Bollobás. Weakly k-saturated graphs. In *Beiträge zur Graphentheorie (Kolloquium, Manebach, 1967)*, volume 25, page 31, 1968.

[6] J. Chalupa, P. L. Leath, and G. R. Reich. Bootstrap percolation on a bethe lattice. *Journal of Physics C: Solid State Physics*, 12(1):L31, 1979.

[7] L. Hambardzumyan, H. Hatami, and Y. Qian. Lower bounds for graph bootstrap percolation via properties of polynomials. *Journal of Combinatorial Theory, Series A*, 174:105253, 2020.

[8] G. Pete. *Disease processes and bootstrap percolation.* PhD thesis, Thesis for diploma at the Bolyai Institute, Jzsef Attila University, Szeged, 1997.